CHAPTER TWELVE

STRESS ANALYSIS FOR THE TORSIONAL MOMENT COMPONENT OF INTERNAL LOADS

Introduction

If we examine a typical heavy-duty power transmitting device, it is likely that a round shaft carrying a large torque is the critical member in designing against yielding. Moreover, the size of this shaft and its bearings will usually establish the proportions which govern the sizes of adjacent components and members. Thus it is important that such shafts be appropriately sized, not too small nor too large. This Chapter develops the torsional stress analysis background relevant to the sizing methodology presented in Chapter 14.

We also examine stress concentration, residual stress, and torsional stress analysis for noncircular members in this Chapter.

NOMINAL STRESS DISTRIBUTION FOR ROUND MEMBERS

We may establish the deformation within a long slender member being twisted by simple reasoning only if the member has a round (circular) cross section. Otherwise the deformations are too complex, and advanced analysis is required.

Figure 12.1 may be used to establish the relevant deformations and strains for round members. The typical segment, as for a tension specimen, is defined by parallel planar surfaces before and after deformation. Moreover, each radial line before deformation remains radial (although rotated) after deformation. No other deformation satisfies geometric compatibility. Accordingly, the shear strains e_{zr} and $e_{r\theta}$ must equal zero everywhere and the shear strain $e_{z\theta}$ may be expressed as

$$e_{z\theta} = (r d\theta)/dz$$

This shear strain is clearly linear in r and takes on its maximum value when $r = r_o$, the outside radius of the round member. We have no information regarding the normal strains e_{rr}, $e_{\theta\theta}$, and e_{zz} except to note that there can be no θ or Z variation for these strains and that $e_{\theta\theta}$ and e_{zz} can have no R variation.

Next consider the stress-strain relationships.

Figure 12.1 Deformation of a typical segment of a round member with a uniform cross section experiencing torsion. A typical radial line on one cross section remains straight and rotates through an angle de relative to the corresponding radial line on the opposite cross section. A typical longitudinal line forms a portion of a helix when the member is twisted.

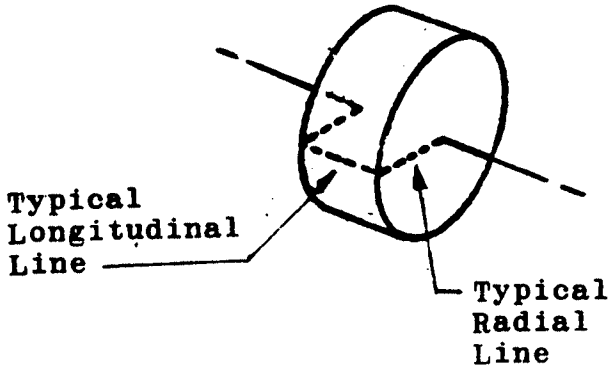

(a) Undeformed Typical Segment

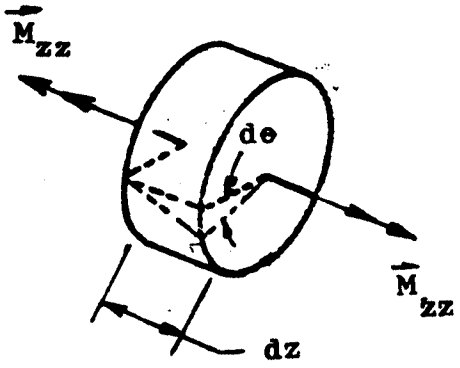

(b) Deformed Typical Segment

Assuming that the material of interest may reasonably be modeled as linear elastic and isotropic, in addition to being homogeneous, we may subsequently use the generalized Hooke's law expressions to write

$$S_{z\theta} = G(r d\theta/dz) \qquad S_{zr} = 0 = S_{r\theta}$$

(noting that $S_{z\theta}$ is linear with respect to r, the radial coordinate location) and

$$e_{rr} = \frac{1}{E}[S_{rr} - \upsilon(S_{\theta\theta} + S_{zz})]$$

$$e_{\theta\theta} = \frac{1}{E}[S_{\theta\theta} - \upsilon(S_{rr} + S_{zz})]$$

$$e_{zz} = \frac{1}{E}[S_{zz} - \upsilon(S_{rr} + S_{\theta\theta})]$$

in which S_{rr}, $S_{\theta\theta}$, and S_{zz} are unknown at present. By analogy with the engineering mechanics solutions for tension and bending, we shall assume these three normal stresses equal zero, and consequently so are the respective normal strains. This assumption leaves only $S_{z\theta}$ to be established by equilibrium analysis.

Static Equilibrium:

Now consider static equilibrium. In Figure 12.2 we see

Figure 12.2 Free body diagram (a) for static equilibrium analysis, with relevant stress information given in (b) and (c).

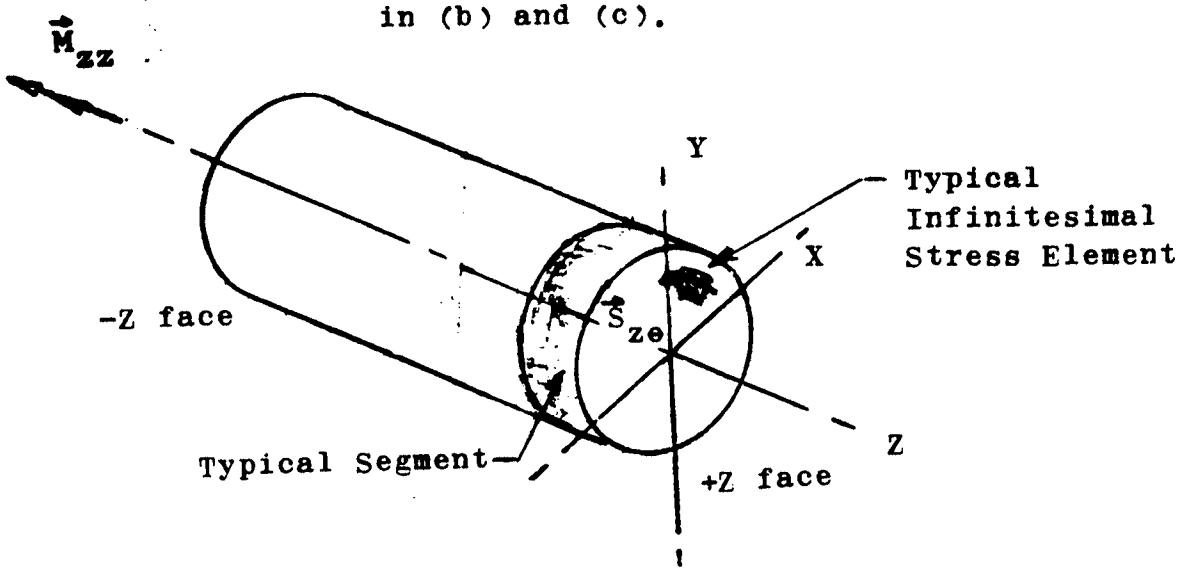

(a) Free body diagram of round member experiencing only torsion along its length.

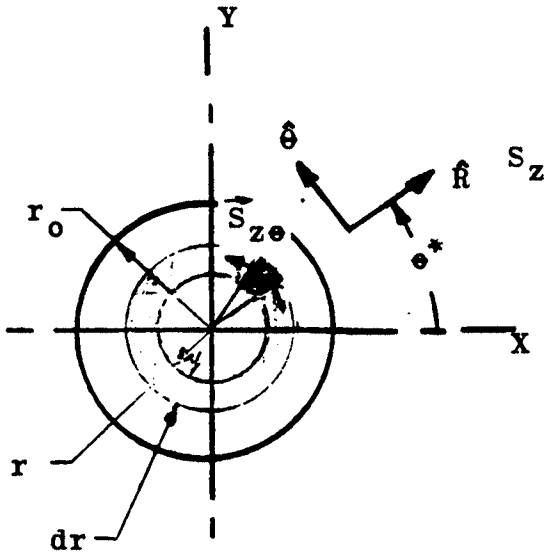

(b) Cross section with shear stress $\vec{S}_{z\theta}$ acting on typical infinitesimal stress element

$S_{z\theta} = (\frac{r}{r_o})S_{z\theta,max}$ $S_{z\theta} = S_{z\theta,max}$ at $r=r_o$

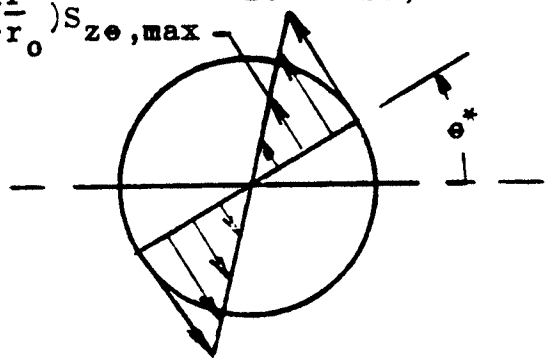

$S_{z\theta}$, magnitude exhibits no θ variation. (Thus, $\Sigma \vec{F} = \vec{0}$ by inspection.)

(c) Linear nominal shear stress distribution (expressed in the form given for convenience in equilibrium analysis)

that $\Sigma \vec{F} = \vec{0}$ is satisfied by inspection, but to satisfy $\Sigma \vec{M} = \vec{0}$, M_{zz} and $S_{ze,max}$ must be related such that

$$(\Sigma \vec{M}) \cdot \hat{z} = 0 = -M_{zz} + \int_0^{r_o} r\left[\left(\frac{r}{r_o}\right) S_{ze,max}(2\pi r dr)\right]$$

Thus,

$$M_{zz} = \frac{\pi r_o^3}{2} S_{ze,max}$$

Solving for the maximum value of the nominal shear stress, $S_{ze,max}$, (which occurs at the outside radius r_o) we obtain

$$S_{ze,max} = \frac{2M_{zz}}{\pi r_o^3}$$

The nominal torsional shear stress distribution is given by the expression

$$S_{ze} = \left(\frac{r}{r_o}\right) S_{ze,max} = \frac{2M_{zz}r}{\pi r_o^4}$$

But recognizing the quantity $(\pi r_o^4/2)$ as I_{RR}, the polar moment of inertia of the round cross sectional area, the nominal torsional shear stress distribution may be re-expressed as

$$S_{ze} = \frac{M_{zz}r}{I_{RR}} \qquad [12.1]$$

Twist Angle:

We may establish the twist angle for the typical segment in Figure 12.2 using the expression

$$S_{z\theta} = G(r d\theta/dz)$$

First, we write

$$G(d\theta/dz) = S_{z\theta}/r = M_{zz}/I_{RR}$$

and then we solve for $d\theta$ to obtain

$$d\theta = (M_{zz}/GI_{RR})dz$$

in which $d\theta$ is the twist angle for the typical segment of length dz. If, for the internal load diagram of interest, the twisting moment (torque) is constant along a particular length, the total twist (in radians) pertaining to that length is

$$\Delta(\theta) = [\frac{M_{LL}}{GI_{RR}}]\Delta(L)$$

This twist angle may be surprisingly large even though shear modulus G is on the order of 70 Gpa (but $d\theta/dz$ must be small for the solution herein to agree with elasticity theory).

Mohr's Circle Analysis:

Since the nominal torsional shear stress distribution is linear for round members, the stress element of interest in a Mohr's circle analysis lies at the surface of the member, Figure 12.3(a). Static equilibrium analysis for the portion of a typical segment in (c) shows that

$$(\Sigma \vec{F})\cdot\hat{N} = 0 = + \int_{A_n} S_{nn}\,dA_n(\hat{N}\cdot\hat{N}) + \int_{A_z} S_{z\theta}\,dA_z(-\hat{\theta}\cdot\hat{N}) + \int_{A_\theta} S_{\theta z}\,dA_\theta(\hat{Z}\cdot\hat{N})$$

$$= S_{nn}A_n + S_{z\theta}A_z\sin\phi + S_{\theta z}A_\theta\cos\phi$$

and

$$(\Sigma \vec{F})\cdot\hat{T} = 0 = + \int_{A_n} S_{nt}\,dA_n(\hat{T}\cdot\hat{T}) + \int_{A_z} S_{z\theta}\,dA_z(-\hat{\theta}\cdot\hat{T}) + \int_{A_\theta} S_{\theta z}\,dA_\theta(\hat{Z}\cdot\hat{T})$$

$$= S_{nt}A_n + S_{z\theta}A_z\cos\phi - S_{\theta z}A_\theta\sin\phi$$

But, $A_z = A_n\cos\phi$, $A_\theta = A_n\sin\phi$, and $S_{z\theta} = S_{\theta z}$. Thus,

$$S_{nn} = -S_{z\theta}(2\sin\phi\cos\phi) = -S_{z\theta}\sin(2\phi)$$

Figure 12.3 Mohr's circle analysis. See also Figure 12.4.

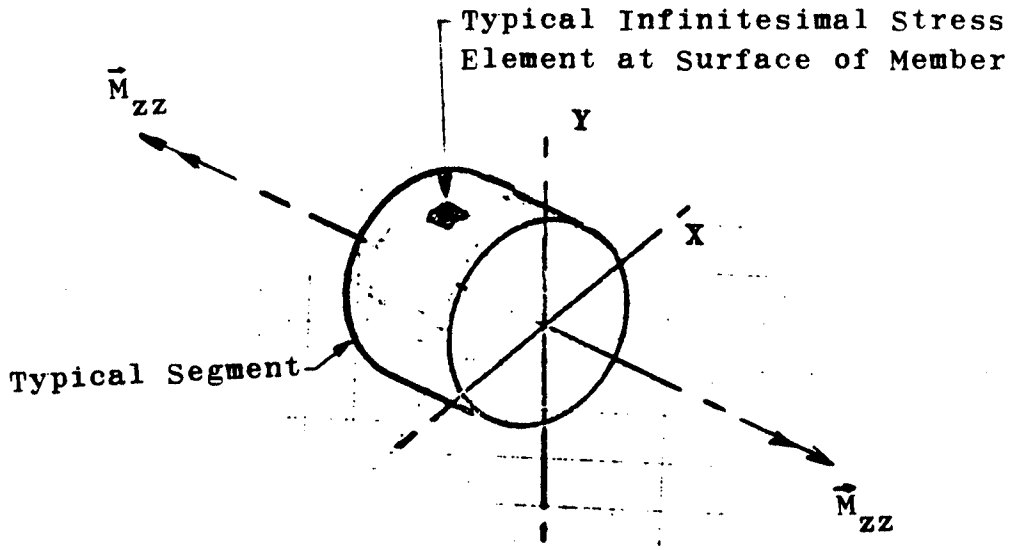

(a) Infinitesimal stress element of interest in a Mohr's circle analysis for torsion.

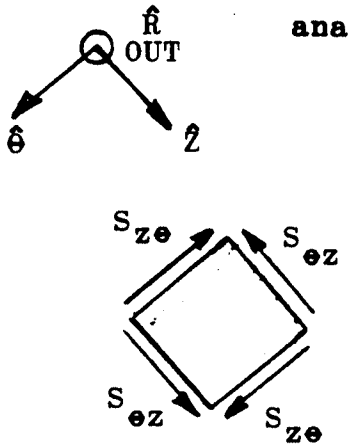

(b) View of typical infinitesimal stress element looking down the $\hat{R}$ unit vector. This element will be shown in three-dimensional perspective later.

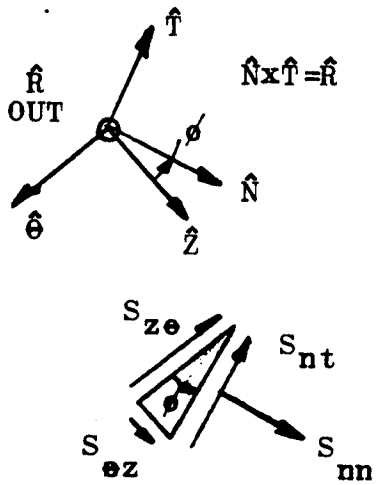

(c) Portion of typical stress element used in static equilibrium analysis.

and

$$S_{nt} = S_{ze}(\sin^2\phi - \cos^2\phi) = -S_{ze}\cos(2\phi)$$

Squaring both expressions and adding gives the equation of a Mohr's circle on S_{nn},S_{nt} coordinates, viz.,

$$S_{nn}^2 + S_{nt}^2 = S_{ze}^2$$

Clearly the center lies at [0, 0] and the radius is equal to S_{ze}, Figure 12.4.

The Mohr's circle for torsion in Figure 12.4(a) shows that the principal stresses act at ϕ = 45 degrees to the coordinate axes. Sketch (b) shows the element in its coordinate orientation (dashed lines) and in its principal orientation (solid lines). Sketch (c) shows the infinitesimal stress element in its principal orientation when S_{33} = 0 is also considered. Looking down each principal axis in turn provides three two-dimensional views of the element in its principal orientation, each of which corresponds to a Mohr's circle in sketch (d). Here we see that the maximum shear stress associated with the three principal stresses is $S_{1/2}$.

Preliminary plot (a) cannot be accepted in design analysis because the third principal stress has not been adequately considered. Rather, design analysis requires a plot of the form in sketch (d), viz., three superimposed two-dimensional Mohr's circles, each associated with a different pair of principal stresses.

Figure 12.4 Mohr's circle for torsion.

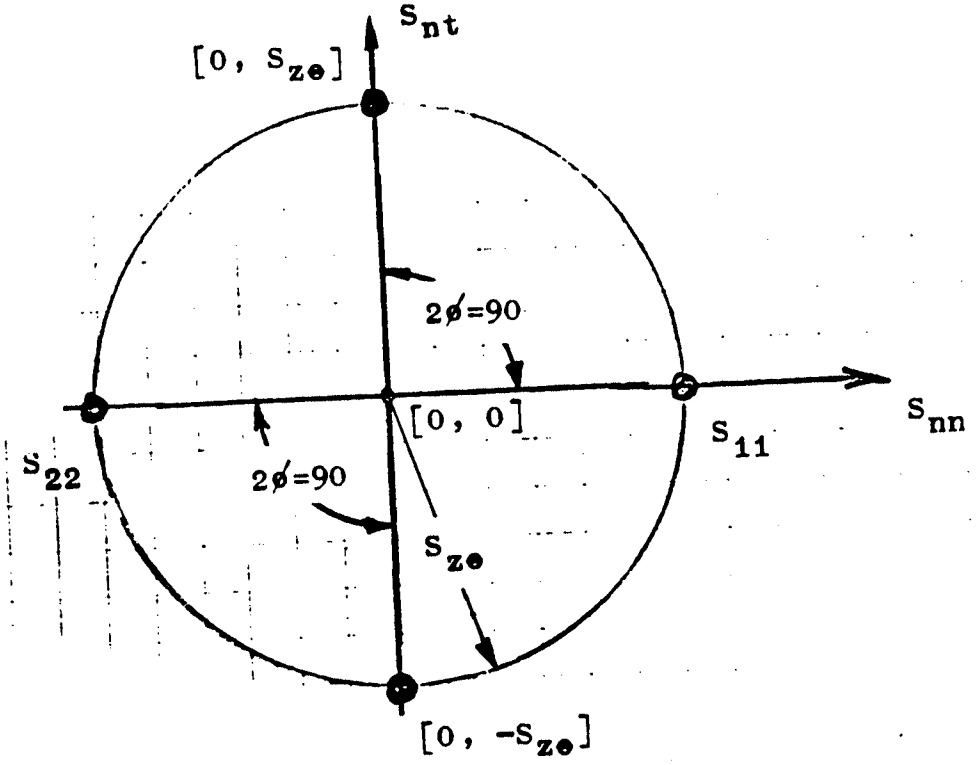

(a) Preliminary plot of Mohr's circle. The stresses acting on the coordinate faces in Figure 12.3(b) plot at coordinates $[0, S_{z\theta}]$ for $\phi=0$ and at $[0, -S_{z\theta}]$ for $\phi=90$.

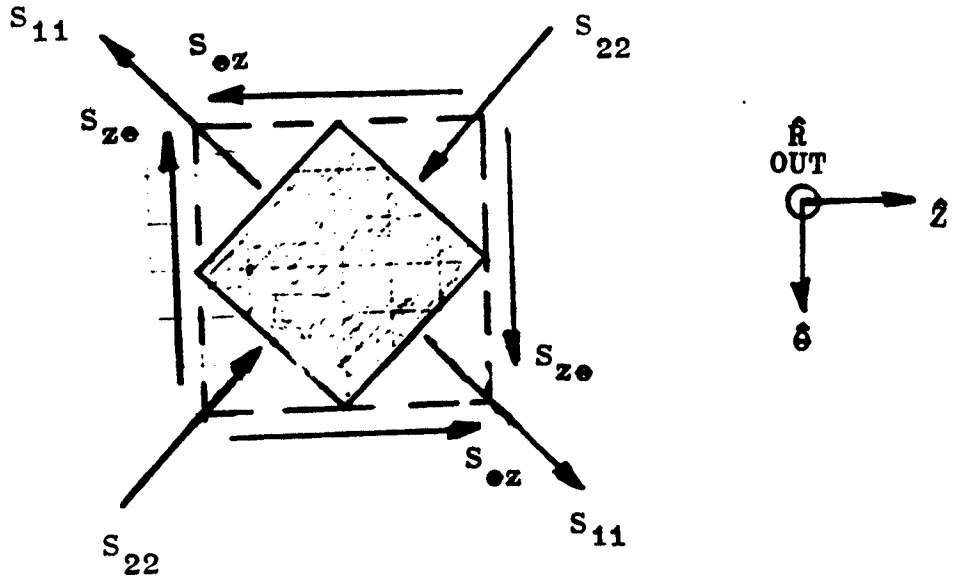

(b) Equivalent states of stress: element in coordinate orientation (dashed lines) and in principal orientation (solid lines).

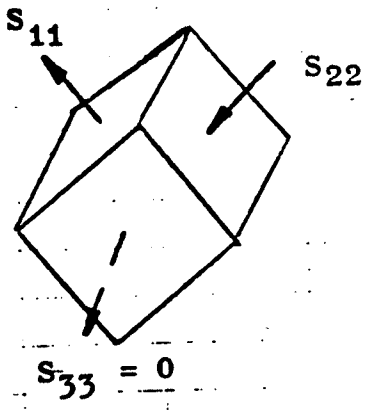

(c) Infinitesimal stress element in its principal orientation. Looking down each principal axis in turn generates three two-dimensional sketches of the element.

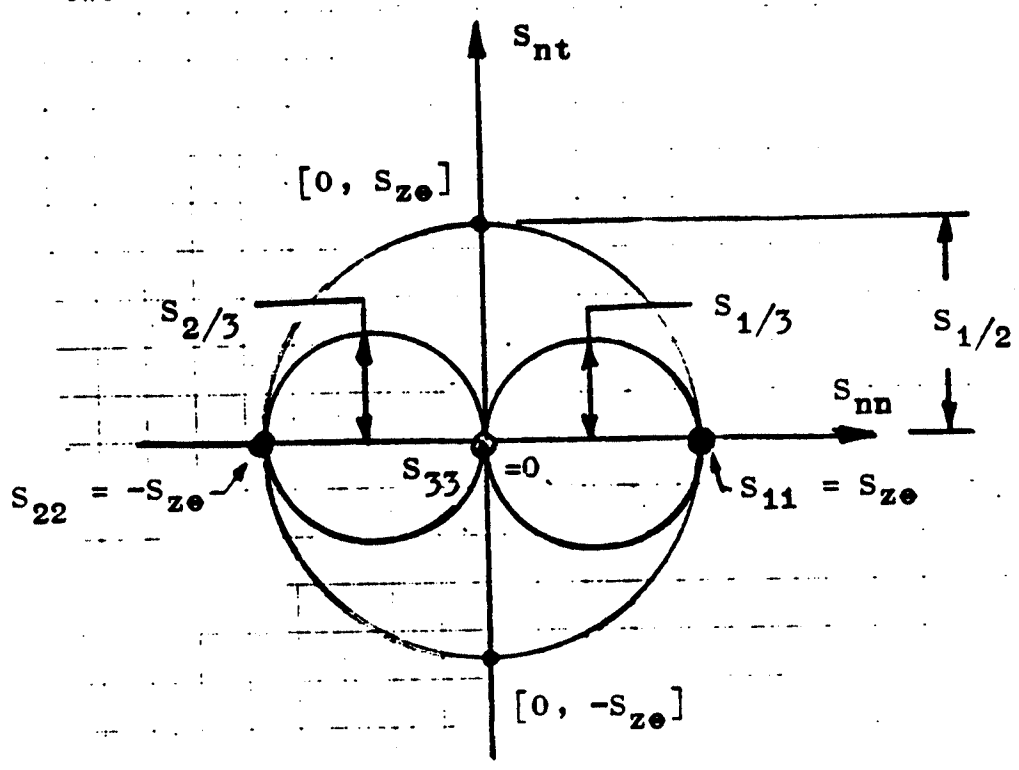

(d) Mohr's circles for torsion. The maximum shear stress pertains to the S_{11}, S_{22} Mohr's circle.

THE TORSION TEST

The torsion test provides information about material behavior under a biaxial state of stress (as opposed to a uniaxial state of stress for a tension test). However, the analysis of a torsion test is not quite as straightforward as the analysis of a tension test. The associated problems warrant discussion.

We begin our discussion of a torsion test analysis by considering a round solid specimen and assuming that the material of interest may reasonably be modeled as being elastic, perfectly plastic. The relevant shear stress-strain diagram appears in Figure 12.5(a). The associated shear stress distribution in a torsion specimen twisted until yielding occurs to depth r_Y is shown in (b). (Compare this shear stress distribution with that in Figure 12.2(c).)

Figure 12.6 shows the associated torque-twist plot for the torsion specimen. The point $M_{zz,e}$ pertains to the maximum twisting moment (torque) before yielding occurs. The value $M_{zz,c}$ is termed the collapse torque. It corresponds to yielding all the way to the center of the member.

The point $[M_{zz,e}, \theta_Y]$ on the torque-twist diagram is located at

$$M_{zz,e} = \frac{S_{nt,Y,torsion}\, I_{RR}}{r_o} \qquad \theta_Y = \frac{S_{nt,Y,torsion}\, L}{G r_o}$$

Figure 12.5 (a) Elastic, perfectly plastic stress-strain diagram to describe the behavior of an infinitesimal element in a torsion test specimen. (b) Shear stress distribution in a round torsion specimen when yielding has occurred (assuming an elastic, perfectly plastic material) to a depth defined by radius r_Y.

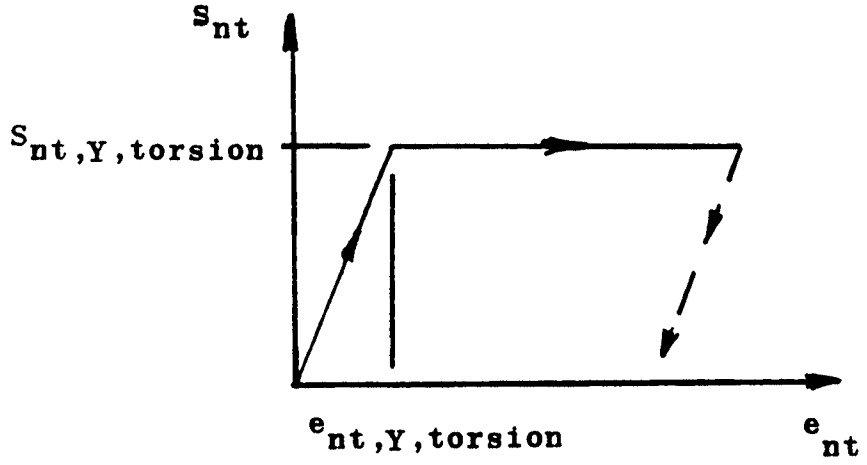

(a) Elastic, perfectly plastic shear stress-strain diagram

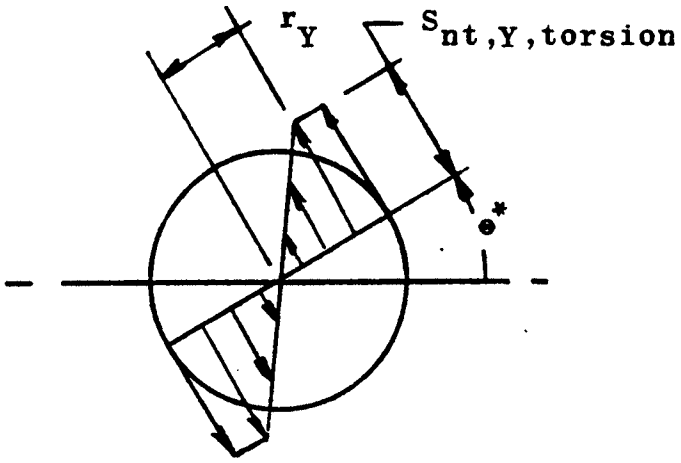

(b) Associated shear stress distribution for yielding to depth r_Y. Compare to Figure 12.2(c).

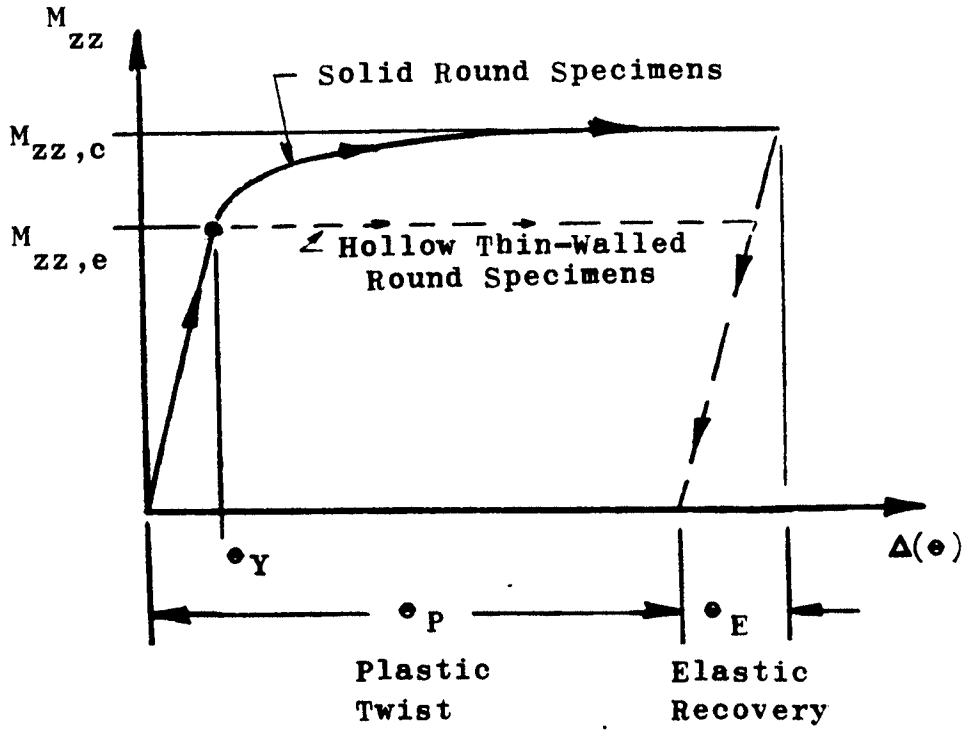

Figure 12.6 Torque-twist angle (in radians) plot for a round solid specimen (solid line) twisted until yielding occurs (overstrained) and then unloaded. Note that a different plot occurs when a hollow specimen is tested. (Moreover, even a different curve for the solid specimen would be observed if it started out with residual stress, rather than being stress-free as assumed above.)

Further twisting causes the specimen to yield. Subsequent twist angles are related to the depth of yielding by the relationship

$$\Delta(\theta) = \left(\frac{r_o}{r_Y}\right)\theta_Y$$

(because the strain distribution is assumed to be linear regardless of the stress-strain model subsequently adopted in analysis). The associated twisting moment corresponding to yielding to radius r_Y is

$$M_{zz} = \int_0^{r_Y} [r[\left(\frac{r}{r_Y}\right)S_{nt,Y,torsion}](2\pi r dr) + \int_{r_Y}^{r_o} r[S_{nt,Y,torsion}](2\pi r dr$$

$$= \frac{2\pi}{3} S_{nt,Y,torsion} r_o^3 [1 - \frac{1}{4}\left(\frac{r_Y}{r_o}\right)^3]$$

Thus,

$$M_{zz} = \frac{2\pi}{3} S_{nt,Y,torsion} r_o^3 [1 - \frac{1}{4}\left(\frac{\theta_Y}{\Delta(\theta)}\right)^3]$$

This expression is used to plot the torque-twist diagram from point $M_{zz,e}$ to the twist angle $\Delta(\theta)$ of interest. Observe that as $\Delta(\theta)/\theta_Y$ becomes relatively large, M_{zz} approaches the limiting value $M_{zz,c} = (4/3)M_{zz,e}$. This point is emphasized by rewriting the torque-twist angle relationship in the form

$$M_{zz} = \frac{4}{3} M_{zz,e} \left[1 - \frac{1}{4} \left(\frac{\theta_Y}{\Delta(\theta)} \right)^3 \right]$$

Exercise:

Conduct a detailed development of the torque-twist angle relationship assuming that yielding occurs according to the shear stress criterion and plot the resulting relationship for r_o = 12mm, L = 100mm, G = 70 Gpa, and $S_{Y,tension}$ = 450 Mpa.

Yielding:

The torque-twist angle plot in Figure 12.6 for a solid specimen is analogous to a load-elongation plot for a tension test specimen with a material that exhibits continuous (as opposed to discontinuous) yielding -- even though an elastic, perfectly plastic material was assumed in developing the torque-twist angle relationship. Accordingly, it is commonly recommended that hollow thin-walled round specimens be used in torsion tests. (But care must be taken in establishing the dimensions of the torsion specimen to prevent buckling under subsequent twisting.) Nevertheless, most existing data pertain to solid specimens, and it is likely that the associated yield strengths reported in the literature are slightly biased on the high side unless some analytical correction was made to compensate for the "raised"

yield strength in torsion (and in bending and combined stress) tests on solid specimens.

Exercise:

Use the torque-twist angle plot in the Exercise above to generate a shear stress-strain plot and then determine the 0.2% offset yield strength (ASTM E8-78). What is the percentage error.

Figure 12.7 shows a "design curve" which may be used to estimate the torsional yield strength of constructional steels (viz., with ultimate tensile strengths less than about 1400 Mpa) when no other information is available, e.g., in preliminary design. Note that the ratio of the torsional to tensile yield strength depends on the material processing. Insufficient data exist for other materials to present similar plots. However, the literature contains enough relevant data in most design applications to justify a literature search and subsquent reading of selected papers.

Exercise:

Conduct a literature search for the tensile and torsional yield strengths of a Ni-Cr alloy steel heat-treated to a Rockwell C hardness between, say, 45 and 55, and compare the ratio to that estimated using the design curve in Figure 12.7.

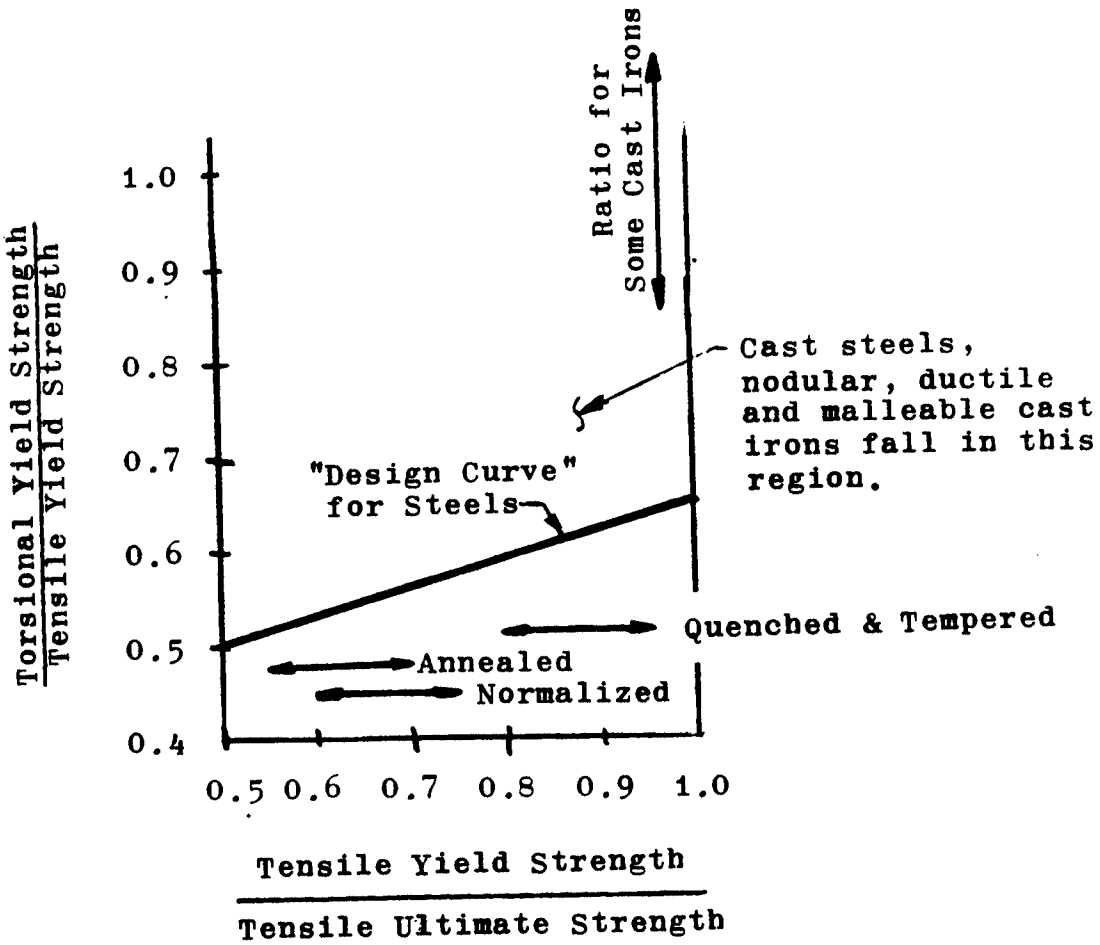

Figure 12.7 "Design curve" to estimate the torsional yield strength of a constructional steel (tensile ultimate strength less than 1400 Mpa) when no better information is available. Whenever possible, data pertaining to the given material, processing, mode and rate of loading, environment, etc. should be used in design analysis.

Residual Stress:

Consider again the shear stress-strain plot in Figure 12.5(a) for an elastic, perfectly plastic material. Regardless of the magnitude of the prior plastic strain, unloading occurs elastically (until a strain $e_{nt,Y,torsion}$ of the opposite sense is reached). Accordingly, the entire torsion specimen unloads elastically as shown in Figure 12.6 (along a line parallel to the initial elastic loading line). Figure 12.8 displays the relevant stress distributions during the unloading process and the resulting residual stress distribution.

Exercises:

1. Explain how the naive factor of safety for a torsion bar in an automotive application can be increased by introducing residual stress by overstraining during fabrication. (What precautions are relevant.)

2. Construct a Mohr's circle for the residual stress state in Figure 12.8 and describe the principal state of residual stress.

3.** Suggest a way that the naive factor of safety could be modified to account for residual stress.

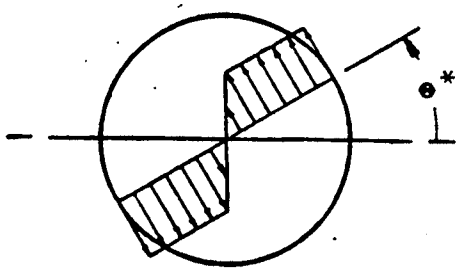

(a) Stress distribution with yielding caused by applied moment $\vec{M}_{zz}$. (Compare with Figure 12.5(b).)

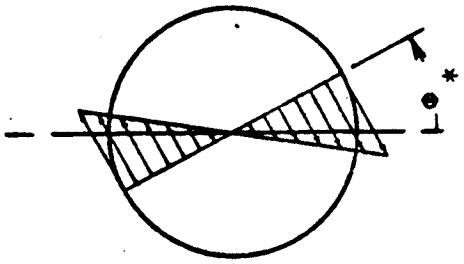

(b) Elastic unloading stress distribution (associated with an unloading moment $-\vec{M}_{zz}$ which negates the applied moment $\vec{M}_{zz}$).

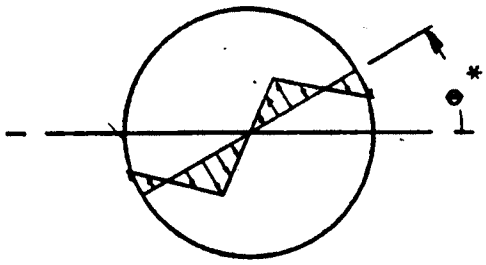

(c) Residual stress distribution (equals (a) - (b)). No applied moment.

Figure 12.8 Analytical development of the residual stress distribution associated with yielding of an initially stress-free round member by overstraining in torsion.

STRESS CONCENTRATION FACTORS

The engineering mechanics expression [12.1] for nominal torsional shear stress finds application in design analysis when it is appropriately modified to account for stress concentration. Figure 12.9 pertains to torsion of long slender straight members with circular cross sections. For fillets and grooves the infinitesimal stress element associated with each stress concentrator experiences only shear stresses in its coordinate orientation. Hence the Mohr's circles for local stress are identical to the Mohr's circles in Figure 12.4 except for a scale factor (viz., the stress concentration factor). But for a cross hole, the state of stress is more complex and the maximum principal stress is associated with the circumferential or hoop stress around the hole itself. Hence, we use the general expression to compute the maximum local principal stress

$$S_{pp,max} = K_{t,pp} S_{pp,nom} \qquad [9.2(a)]$$

in which $S_{pp,nom}$ is equal to $S_{ze,nom}$ (at the outside surface of the round member) as evident in Figure 12.4(d). This stress concentration factor is academic in the sense that it applies only to a simple mode of loading, but it has the inherent problem that to use it to construct an applied stress concentration factor for combined loads we must be careful to assure that the local stress information actually pertains to the same location on the stress concentrator. Often this involves using the information upon which the academic stress concentration factor is based, rather than the stress concentration factor itself.

Figure 12.9 Stress concentration factors for torsion. (Care must be taken in defining and using these factors. See text for discussion.)

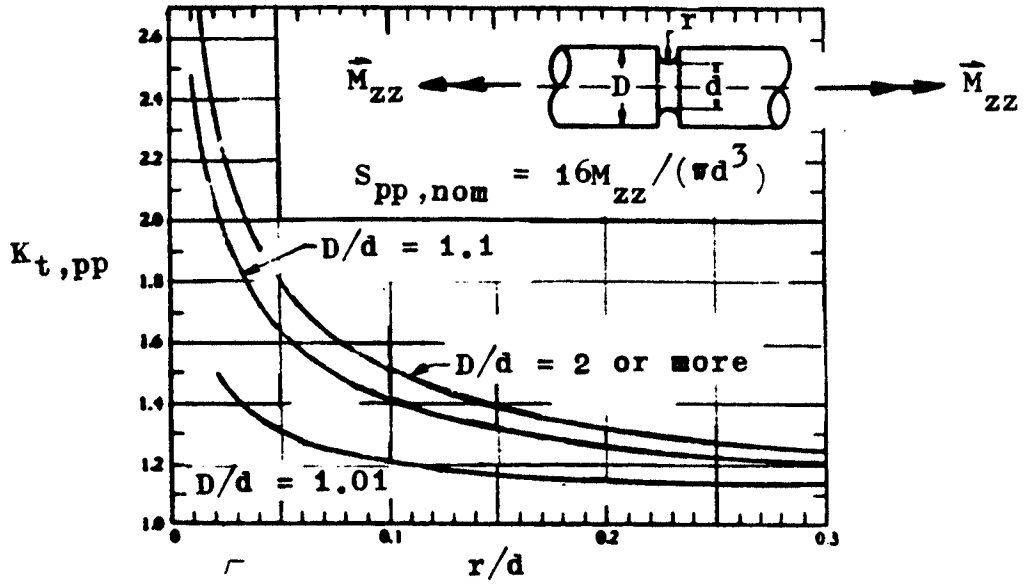

(a) Grooves

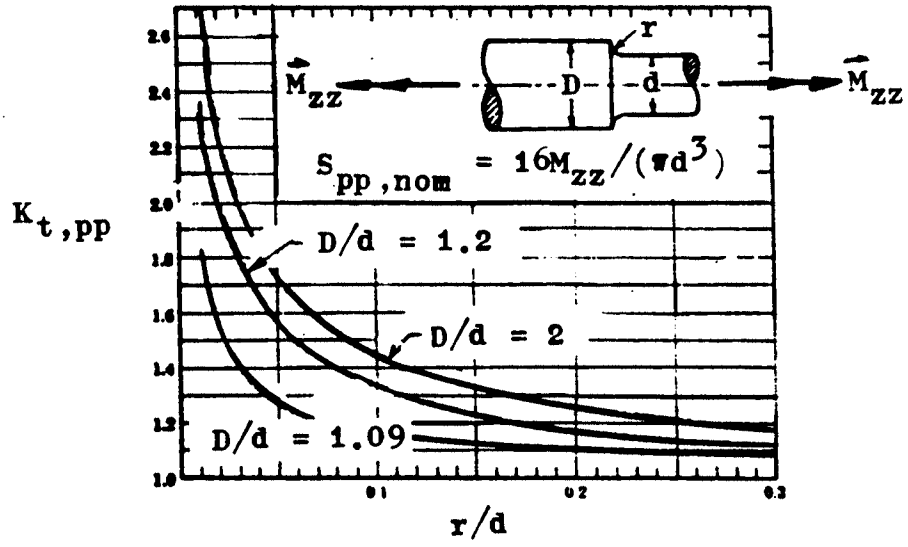

(b) Fillets

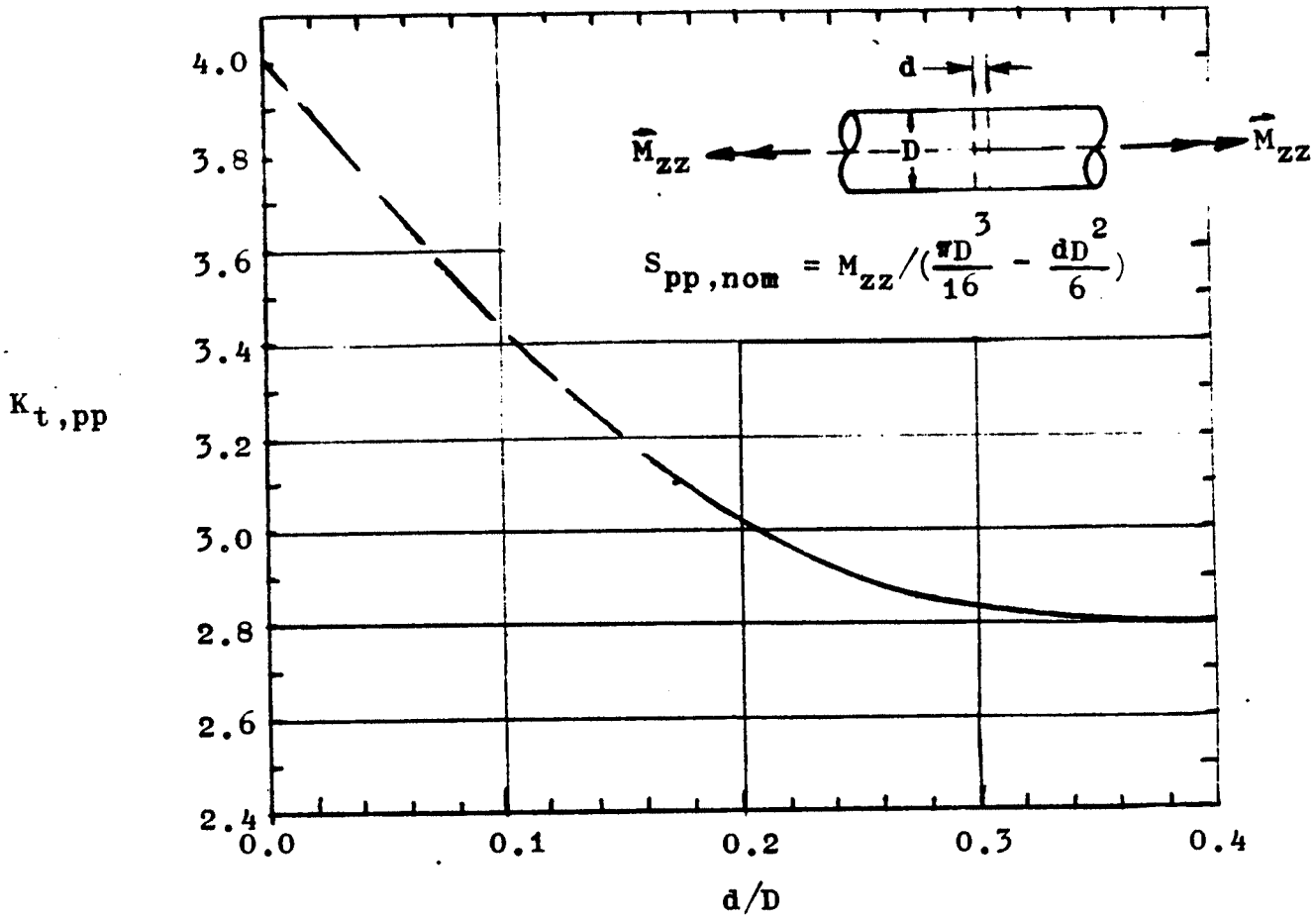

(c) Cross Holes

Note: The maximum principal stress is a circumferential or hoop stress associated with the cross hole d. It occurs down inside the cross hole, approximately D/10 below the surface of the member, at two points 180 degrees apart circumferentially, each of which are at 45 degrees to the plane of the paper. The solid portion of the curve is based on two datum points by Thum and Kirmser about thirty-five years ago using obsolete apparatus. The dashed portion of the curve extrapolates the experimental results to the "theoretical" value of four based on the Kirsch solution and the equivalent principal stress state for torsion.

HELICAL COMPRESSION SPRINGS (CURVED MEMBERS)

The following torsional stress analysis is akin to the bending stress analysis for curved members in Chapter 10.

Figure 12.10 shows a helical compression spring with squared and ground ends, wound from round wire. This sketch also shows the primary internal loads acting on a typical conceptual cross section: torsion, and a shear force component (the axial force component and bending are neglected for small pitch angles).

In Figure 12.11 we examine the geometry of a typical segment of the wire and specify the deformation of a typical filament within the segment. Again, as for bending of curved members, the filament length depends on its location. In (a) we see that $dL = Rd\theta$. Thus, in (c) it is evident that $e_{\theta\phi}$ may be written as

$$e_{\theta\phi} = \frac{\rho d\phi}{Rd\theta}$$

Moreover, if planar surfaces of the typical segment are to remain planar, $e_{\theta\rho}$ must equal zero, and if radial lines remain radial, $e_{\rho\phi}$ must equal zero. But reasoning based on geoemtric compatibility is inadequate to determine the normal strains (althouch cetain constrains could be enumerated). Using the generalized Hooke's law relationships we now write

$$S_{\theta\phi} = G\,\frac{\rho d\phi}{Rd\theta} \qquad S_{\theta\rho} = 0 = S_{\rho\phi}$$

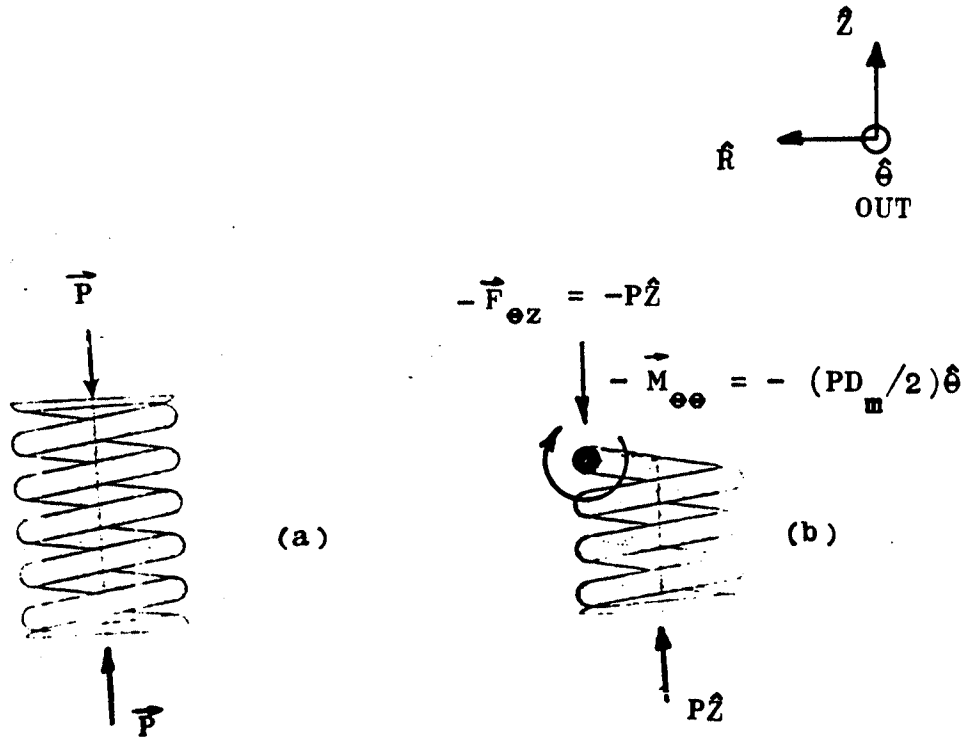

Figure 12.10 Helical compression spring and its primary internal loads: torsion, and a shear force component. The pitch angle λ is ignored in this analysis, viz., we act as if the normal to the conceptual cross section is directed out of the plane of the paper (in the $\hat{\theta}$ direction) rather than upward at angle λ.

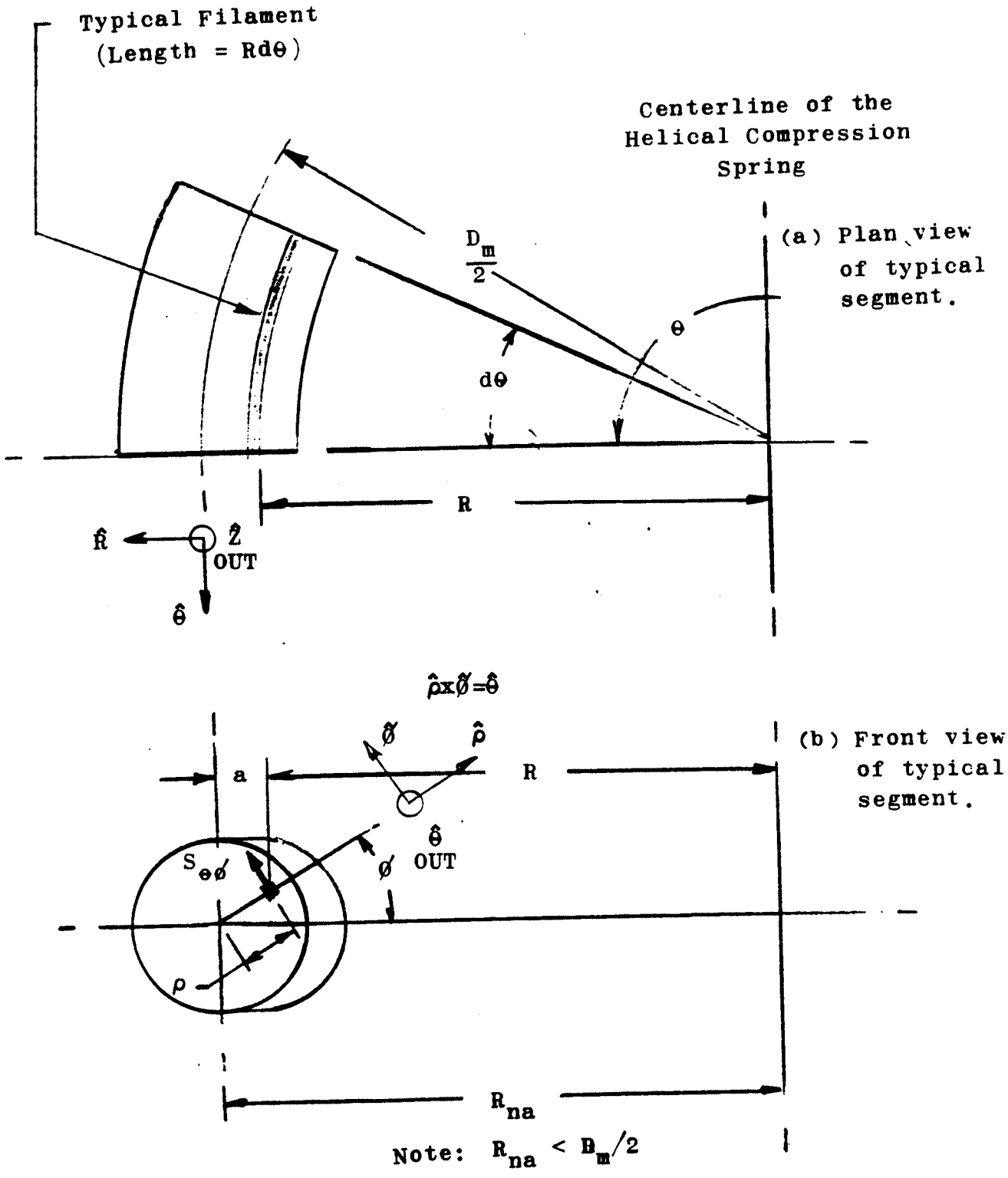

Figure 12.11 Sketches of typical segment and filament, (a) and (b), and of the deformation of the typical filament, (c), used in developing the expression $e_{\theta\phi} = \rho d\phi/Rd\theta$.

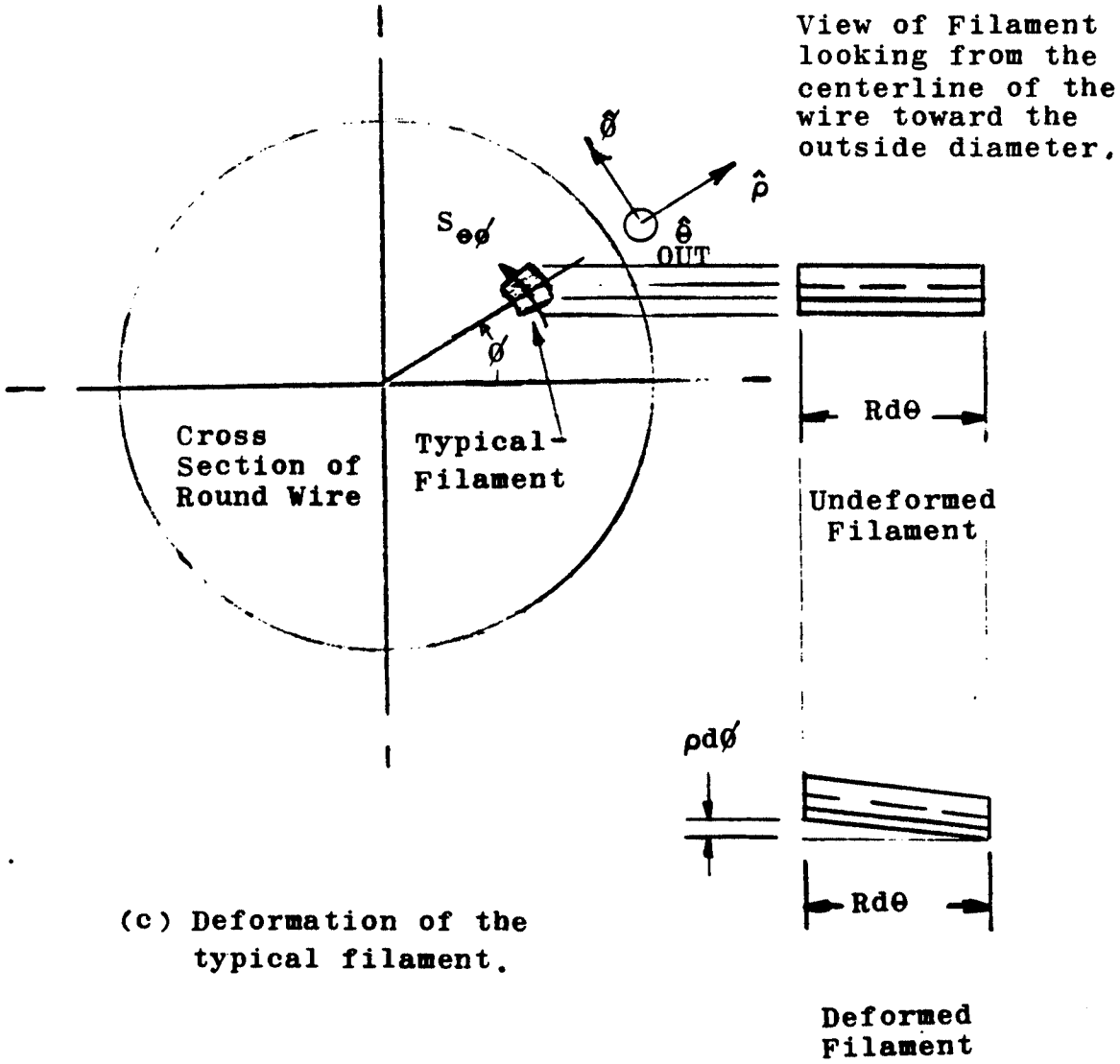

(c) Deformation of the typical filament.

Figure 12.11 Continued

and

$$e_{\rho\rho} = \frac{1}{E}[S_{\rho\rho} - \upsilon(S_{\phi\phi} + S_{\theta\theta})]$$

$$e_{\phi\phi} = \frac{1}{E}[S_{\phi\phi} - \upsilon(S_{\theta\theta} + S_{\rho\rho})]$$

$$e_{\theta\theta} = \frac{1}{E}[S_{\theta\theta} - \upsilon(S_{\rho\rho} + S_{\phi\phi})]$$

Again we must assume that these normal stresses equal zero to permit solution using the engineering mechanics methodology. Thus, only $S_{\theta\phi}$ need be considered in our static equilibrium analysis.

Equilibrium analysis for the typical segment in Figure 12.11(b) is more complex than for previous examples because the neutral axis lies inside the centroid of the wire cross section, i.e., $R_{na} < D_m/2$. Thus the integral

$$\int_A \rho S_{\theta\phi} dA = - P(D_m/2)$$

is difficult to evaluate (because the origin for ρ does not lie at the centroid of the wire cross section). This difficultly may be overcome by adopting the following solution method.

Suppose we consider only the torsional moment $\vec{M}_{\theta\theta}$ and solve for $S_{\theta\phi}$, and next we consider only the shear force component $\vec{F}_{\theta z}$ and solve for, say, $S^*_{\theta\phi}$, and then we add $S_{\theta\phi}$ and $S^*_{\theta\phi}$ at each point of interest. This "superposition" solution method avoids the problem of having to write an integral expression with ρ in the argument. Specifically, we

note that static equilibrium requires that (both)

$$(\Sigma \vec{F})\cdot\hat{Z} = 0 = \int S_{\theta\phi}\cos\phi dA = \int S_{\theta z} dA \quad \text{(Torsion Only)}$$

$$(\Sigma \vec{F})\cdot\hat{Z} = 0 = + P + \int S^{*}_{\theta z} dA \quad \text{(Shear Force Component Only)}$$

and observe that ρ cancels out of the first scalar equation above when we substitute for $S_{\theta\phi}$ and replace $\cos\phi$ by the expression $(R_{na}-R)/\rho$ (Figure 12.11(b)). Thus, to satisfy static equilibrium, we require that

$$\int_A G\left(\frac{d\phi}{d\theta}\right)\left[\frac{R_{na}-R}{R}\right]dA = 0$$

Accordingly, the location of the neutral axis may be computed using the expression

$$R_{na} = \frac{A}{\int_A \frac{dA}{R}}$$

For a round cross section $\int \frac{dA}{R}$ is equal $2\pi\left[\frac{D_m}{2} - \sqrt{\left(\frac{D_m}{2}\right)^2 - \left(\frac{d_w}{2}\right)^2}\right]$ from Table 10.2. When $d_w << D_m$, R_{na} may be computed using the approximate expression

$$R_{na} = \frac{D_m}{2} - \left(d_w^2/8D_m\right)$$

Substituting this approximate expression into

$$S_{\theta z} = G\left(\frac{d\phi}{d\theta}\right)\left[\frac{R_{na}-R}{R}\right] \qquad \text{(Torsion Only)}$$

gives

$$S_{\theta z} = G\left(\frac{d\phi}{d\theta}\right)\left[\frac{\frac{D_m}{2} - \frac{d_w^2}{8D_m} - R}{R}\right] \qquad \text{(Torsion Only)}$$

Refer Figure 12.12(a). $S_{\theta z}$ takes on its maximum value at the inside radius, $R = (D_m/2) - (d_w/2)$. The stress at that point is (assuming that $G(d\phi/dL) = - M_{\theta\theta}/I_{RR}$, where $dL = (D_m/2)d\theta$)

$$S_{\theta z,max} = - \frac{\left(\frac{PD_m}{2}\right)\left(\frac{d_w}{2}\right)}{I_{RR}}\left[\frac{4C - 1}{4C - 4}\right] \qquad \text{(Torsion Only)}$$

in which C is termed the spring index, viz., $C = (D_m/d_w)$. This maximum stress expression may be viewed as being equal to the stress in a straight wire times the Wahl factor $\left[\frac{4C-1}{4C-4}\right]$, Figure 12.13. (The Wahl factor is akin to a stress concentration factor.)

Figure 12.12 Shear stress distributions associated with the torsional and shear force components of the internal loads. The actual shear stress distribution across the horizontal centerline may be viewed as the sum of (a) and (b).

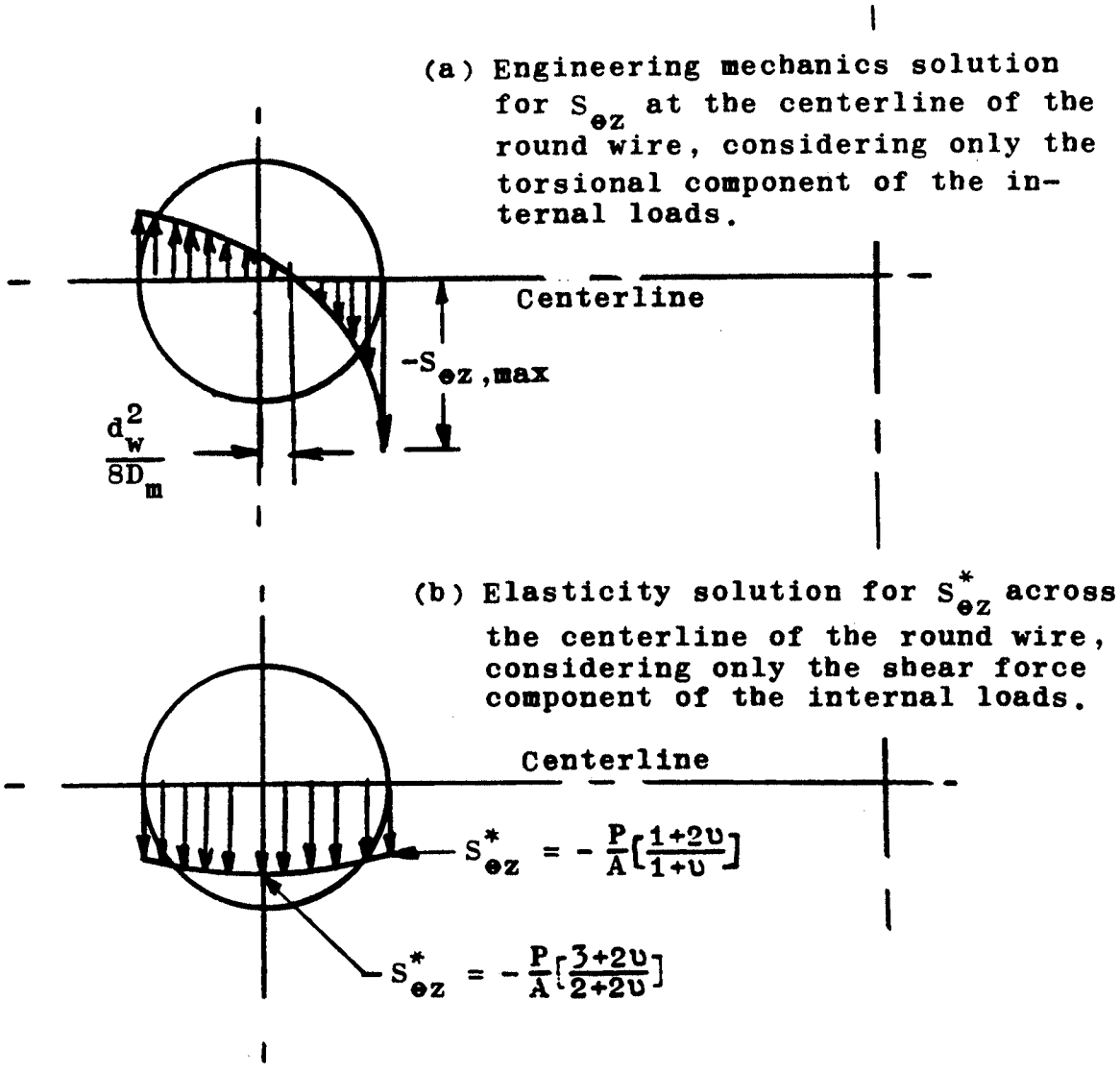

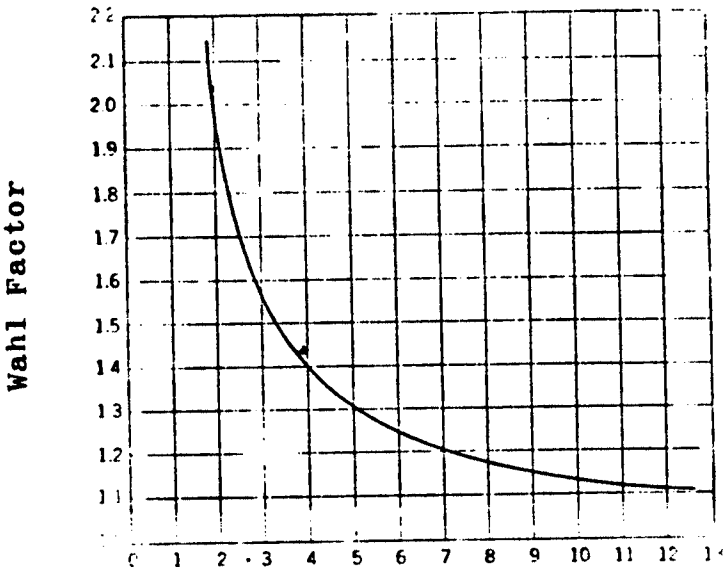

Figure 12.13 Wahl factor for round wire. D_m connotes the mean (average) diameter of the helical compression spring. d_w is the wire diameter.

Exercises:

1.** Verify the approximation for $d_w << D_m$. [Hint: After appropriate algebraic manipulation consider a series expansion of the radical, subsequently neglecting higher order terms.]

2. Verify the expression given for $S_{\theta z,max}$.

3. Show that at the outside radius (and ϕ = 180 degrees)

$$S_{\theta z,min} = \frac{8\,PD_m}{\pi d_w^3}\left[\frac{4C+1}{4C+4}\right] \quad \text{(Torsion Only)}$$

Yielding:

We shall now estimate the maximum load (force) P that can be applied to the spring without causing yielding. In Figure 12.12 we see that the maximum shear stress occurs at the inside diameter and is given by

$$S_{ez,max,total} = - \frac{PD_m d_w}{4 I_{RR}} \left[\frac{4C-1}{4C-4} + \frac{0.615}{C} \right]$$

when υ is taken as 0.3. This shear stress must not exceed $S_{nn,Y,tension}/2$ if the shear stress criterion for yielding is assumed in analysis. Thus,

$$P_{max} = \frac{2S_{nn,Y,tension} I_{RR}}{D_m d_w \left[\frac{4C-1}{4C-4} + \frac{0.615}{C} \right]}$$

Exercises:

1. Given a mean spring diameter of 48mm and a yield strength of 1400 Mpa, what wire diameter is required to prevent yielding when P is as large as 300 Newtons, if a naive factor of safety equal 2.5 is used in design.

2. Show that the term [0.615/C] becomes [0.667/C] when the engineering mechanics expression for transverse shear stress (Equation [11.1]) is used to approximate the shear stress associated with only the shear force component of the internal loads.

Spring Rate and Deflection:

Springs are usually designed to exhibit certain spring rates, viz., to exert certain forces at specific deflections. Thus we now examine the theoretical load-deflection relationship for a helical compression spring. We include the effect of pitch angle herein to provide insight regarding the percentage error when pitch angle is ignored.

The energy stored in the spring is

$$U = \frac{M_{e\theta}^2 L}{2GI_{RR}}$$

where $L = (\pi D_m/\cos\lambda)N_c$ in which N_c is the number of <u>active coils</u>, and $M_{e\theta} = P(D_m/2)\cos\lambda$. Using Castigliano's method,

$$\delta = \frac{dU}{dP} = \frac{8PD_m^3 N_c}{Gd_w^4}\cos\lambda = \frac{8PC^3 N_c}{Gd_w}\cos\lambda$$

Thus the spring rate is

$$K = \frac{P}{\delta} = \frac{Gd_w}{8C^3 N_c \cos\lambda} = \frac{Gd_w^4}{8D_m^3 N_c \cos\lambda}$$

Exercise:**

Consider the bending energy where $M_{ez} = P(D_m/2)\sin\lambda$ and show that

$$\delta = \frac{8PD_m^3 N_c}{Gd_w^4}\left[\frac{1+\upsilon\cos^2\lambda}{(1+\upsilon)\cos\lambda}\right]$$

Plot the percentage error for each expression as a function of λ, $0 < \lambda$ 30 degrees. (Assume the error occurs when λ is neglected.)

Solid Height:

The load (force) P^* that will deflect the spring to its solid height should be at least 20 per cent higher than the maximum design load (force). Otherwise manufacturing variability, particularly in the number of active coils and free length, may cause the spring to "bottom out" in normal service operation. In addition springs should be designed so that the solid height stress does not exceed the yield strength of the material. Figure 12.14 shows the end configurations for helical compression springs. Table 12.1 gives the associated free lengths and solid heights. Tables 12.2 and 12.3 give design data for steel wire.

Exercises:

1. Design a helical compression spring to withstand a maximum force of 1500 Newtons with a deflection of 37.5mm. Let the free length be 175mm and the mean coil diameter be 45mm. Make sure that the maximum value of λ is 12 degrees.

2. A spring having squared and ground ends with an OD equal 48mm is to have a free length of 150mm and a solid height of 100mm. The spring rate required is 125 Newtons/mm. Select and establish:

(a) The wire diameter
(b) The number of active coils
(c) The pitch angle
(d) The maximum shear stress when deflected to solid height.

Design Procedure:

The two design exercises above should indicate clearly the distinct differences between synthesizing dimensions by analytical and subjective means, and merely analyzing a member whose dimensions are known. The former is design, the latter is mechanics. We could present a design methodology for sizing springs, but it appears worthwhile to encourage the student to consider alternative approaches before deciding on a design method. Accordingly, we present a few selected references which may provide some perspective and practical information.

Hinkle and Morse, Design of Helical Springs for Minimum Weight, Volume, and Length", Transactions of the ASME, Journal of Engineering for Industry, February 1959, pp 37-42.

Machine Design:

Johnson and Joerres, "Poor Spring Performance..Its Causes and Cures", August 4, 1966, pp 132-138.

Craig and Kwossek, "Instant Optimization for Springs: Computer Tabulated Characteristics Eliminate Trial and Error Design, September 28, 1967, pp 165-169.

Dilpare, "Where Space is Limited, You Need Maximum-Work Springs", July 4, 1968, pp 111-112.

Chepko, "Taking the Mystery Out of Spring Design", June 25, 1970, pp 144-146.

Skelskey, "The Cost of Springs", May 13, 1971, pp 137-139.

Exercises:

1. Recommend a reference (not given above) on design procedure for helical compression springs.

2. Recommend a reference for obtaining information on the strength of spring materials.

3. Recommend a good general reference on spring design.

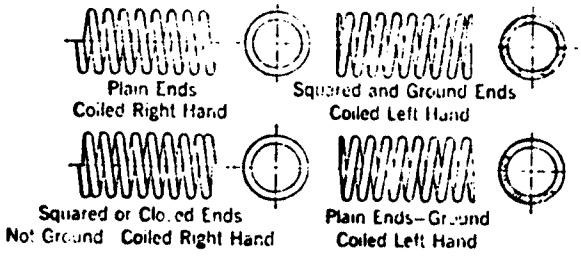

Figure 12.14 End conditions for helical compression springs. Refer Table 12.1 for free lengths and solid heights.

Table 12.1 Free lengths and solid heights for helical compression springs (approximate values).

Notation: p = pitch of coils, N_c = number active coils, d_w = wire diameter

TYPE OF ENDS	TOTAL COILS	FREE LENGTH	SOLID HEIGHT
Plain	N_c	$pN_c + d_w$	$N_c d_w + d_w$
Plain Ground	N_c	pN_c	$N_c d_w$
Squared	$N_c + 2$	$pN_c + 3d_w$	$N_c d_w + 3d_w$
Squared and Ground	$N_c + 2$	$pN_c + 2d_w$	$N_c d_w + 2d_w$

Table 12.2 Available wire sizes for helical compression springs.

W and M Ferrous Gage No.	Wire Diameter, in.
7-0	0.4900
6-0	0.4615
5-0	0.4305
4-0	0.3938
3-0	0.3625
2-0	0.3310
0	0.3065
1	0.2830
2	0.2625
3	0.2437
4	0.2253
5	0.2070
6	0.1920
7	0.1770
8	0.1620
9	0.1483
10	0.1350
11	0.1205
12	0.1055
13	0.0915
14	0.0800
15	0.0720
16	0.0625
17	0.0540
18	0.0475

Table 12.2 Wire sizes for helical compression springs.

W & M Ferrous Gauge Number	Wire Diameter, mm
0000000	12.45
000000	11.72
00000	10.93
0000	10.00
000	9.21
00	8.41
0	7.79
1	7.19
2	6.67
3	6.19
4	5.72
5	5.26
6	4.88
7	4.50
8	4.11
9	3.77
10	3.43
11	3.06
12	2.68
13	2.32
14	2.03
15	1.83
16	1.59
17	1.37
18	1.21

Table 12.3 Maximum allowable solid height stresses. Notation: D_w = wire diameter, S_s = maximum allowable solid height shear stress.

Material (Size Limits)	Max. Stress ksi
Hard-drawn carbon steel ($0.05 < D_w < 0.5$ in.)	$s_s = \frac{60}{D_w^{0.2}}$
Oil-tempered carbon steel ($0.05 < D_w < 0.5$ in.)	$s_s = \frac{77}{D_w^{0.22}}$
Oil-tempered alloy steel ($0.05 < D_w < 0.5$ in.)	$s_s = \frac{105}{D_w^{0.186}}$
Music wire ($0.03 < D_w < 0.15$ in.)	$s_s = \frac{96}{D_w^{0.17}}$
Hard-drawn stainless, 302 ($0.05 < D_w < 0.5$ in.)	$s_s = \frac{60}{D_w^{0.2}}$

TORSIONAL STRESS ANALYSIS FOR NONCIRCULAR MEMBERS

We now briefly consider several topics in the realm of torsional stress analysis for noncircular members.

Closed Thin-Walled Sections:

Consider the thin-walled cylindrical member in Figure 12.15(a). Assume that the member experiences only torsion along its length and that it has an arbitrary cross section with a nonuniform wall thickness. Static equilibrium analysis for the shear flow free body in (b) indicates that the product $S_{xp}(t)$ is a constant, i.e., the shear flow q_{xp} is a constant. In turn, using sketch (c), static equilibrium for (a) requires that

$$(\Sigma \vec{M}) \cdot \hat{x} = - M_{xx} + \int_P r(q_{xp})dp$$

But q_{xp} is a constant and $\int_P rdp = 2A$, where A is the area enclosed by the centerline of the cross section. Hence, $q_{xp} = M_{xx}/(2A)$.

Figure 12.15 Sketches for the development of the expression $q_{xp} = M_{xx}/(2A)$. (a) Member geometry: arbitrary cross section with nonuniform wall thickness. (b) Shear flow free body diagram. (c) Geometry interpretation of r(dp) in the integral evaluated around perimeter P, viz., the area of the triangle shown is (1/2)[r(dp)]. Thus, the integral equals twice the cross sectional area.

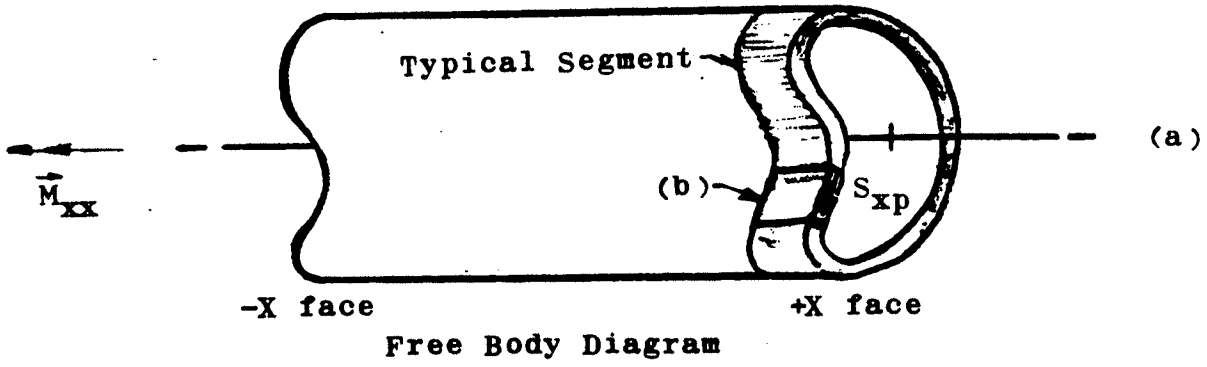

Free Body Diagram

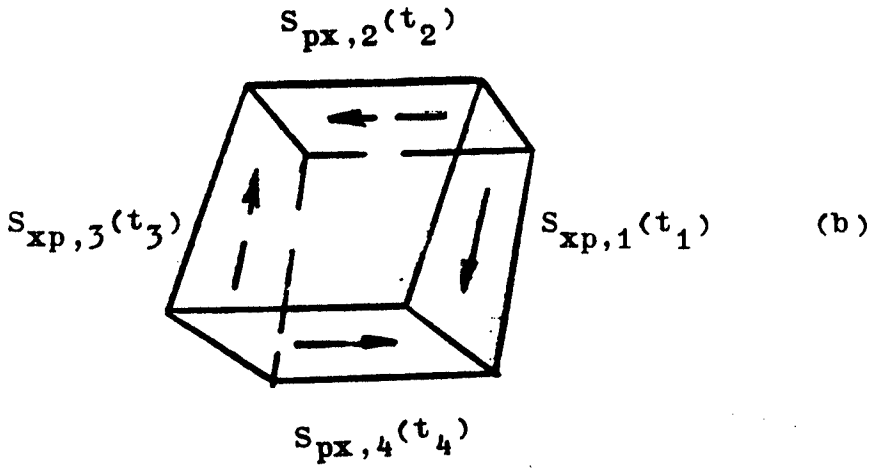

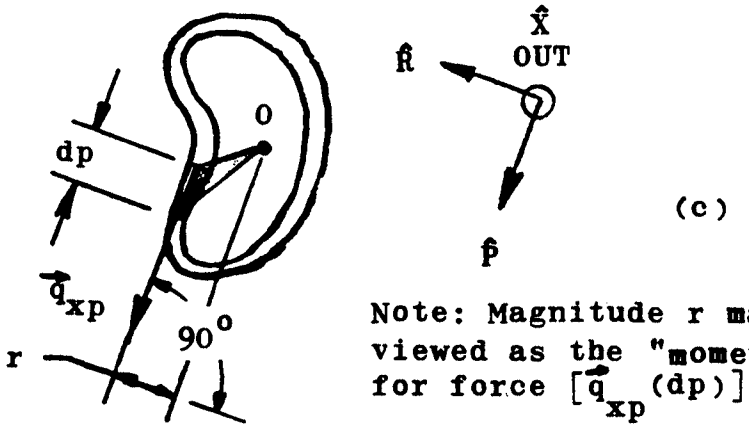

Note: Magnitude r may be viewed as the "moment arm" for force $[\vec{q}_{xp}(dp)]$.

Exercises:

1. Check the accuracy of the expression

$$S_{xp} = \frac{M_{xx}\, t}{2A}$$

when used for a thin-walled <u>round</u> tube by examining the per cent error occurring when this expression replaces that of Equation [12.1]. Suppose you increase S_{xp} by the ratio (r_o/r_m). How does this affect your conclusions.

2. Consider the shear flow free body in (b). For the thin-walled geometry assumed, we can argue that certain stresses are zero (or negligible). In addition, we tacitly assume that certain other stresses are equal to zero. Identify these two sets of coordinate stresses.

3. Argue that $\Sigma \vec{F} = \vec{0}$ for the free body diagram in (a).

Members with Rectangular Cross Sections:

Although torsional stress analysis for members with rectangular cross sections is beyond the scope of this text, we may use arguments based on symmetry to show that the dashed lines displayed in Figure 12.16(b) remain straight after deformation (and also remain perpendicular to the longitudinal axis). Moreover, we know that the shear stresses at each of the corners of the cross section must equal zero -- because the external surfaces of the member are free of both normal and shear stresses, (c). However, we cannot establish the deformations throughout the rectangular cross section by simple reasoning based on geometric compatibility. Rather, we know from examining the deformation of rubber models with small square surface grids (Figure 12.17) that the deformations are relatively complex and that the cross section warps, (i.e., does not remain planar during deformation).

Advanced analysis shows that the maximum shear stress occurs at the surface of the cross section along the central portion of the longer sides of the rectangle. The stress at that point depends on the ratio, a/b. When a/b is very large, S_{xt} may be estimated using the expression

$$S_{xt} = 3\frac{M_{xx}}{ab^2}$$

in which the subscript t infers that the shear stress acts in a direction tangent to the surface in the region where it takes on its maximum value. Figure 12.18. When the ratio a/b is less than about ten to fifteen, S_{xt} may be estimated using the expression

Figure 12.16 A long slender straight member with a rectangular cross section, experiencing only torsion along its length.

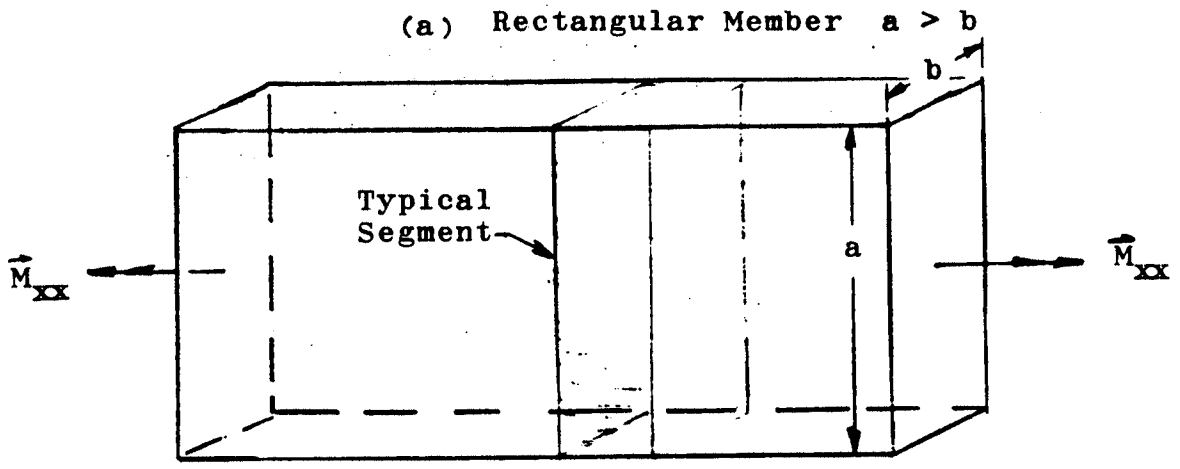

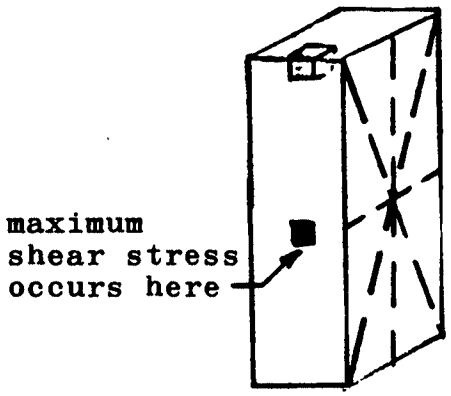

(b) Typical segment, with certain lines indicated on the X face which, by symmetry, must remain straight during deformation. These lines must also remain perpendicular to the X axis.

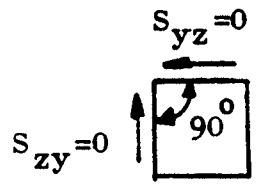

(c) Stress element located at a corner of the cross section. Equilibrium indicates that $S_{yz}=S_{zy}=0$.

Figure 12.17 Schematics of the deformation of rubber models with small square grids during twisting. (a) Uniform deformation for members with circular cross sections. (b)Nonuniform deformation for members with rectangular cross sections.

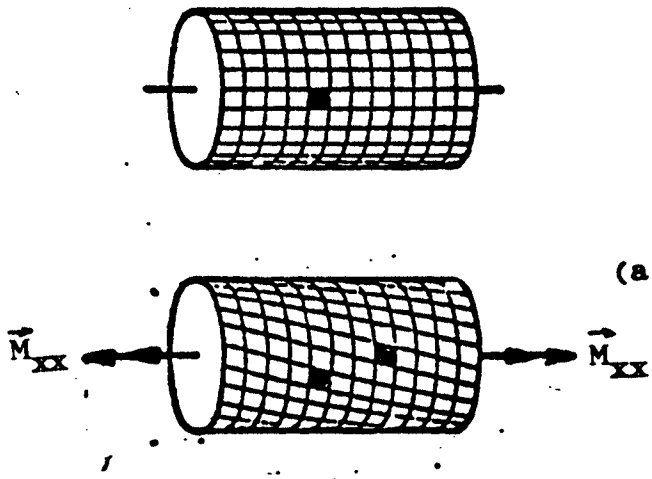

(a)Circular Cross Sections

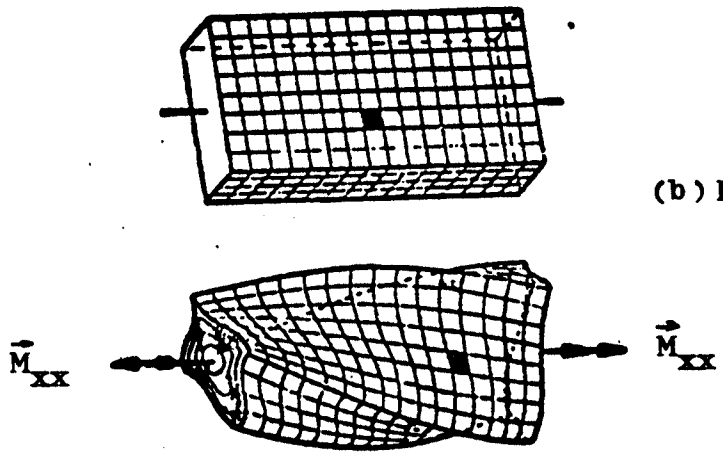

(b)Rectangular Cross Sections

Figure 12.18 Schematic illustrating the shear stress direction and distribution in a long straight member with a rectangular cross section. The shear stress along sides b cannot attain a large value because the stress at the corners is zero. Thus the maximum shear stress occurs along the central portions of the longer sides at the surface.

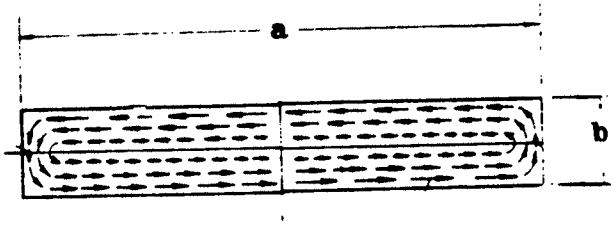

$$S_{xt} = [3 + 1.8/(a/b)]\frac{M_{xx}}{ab^2}$$

Members with Open Thin-Walled Cross Sections:

The analysis for members with rectangular cross sections may be extrapolated to estimate (crudely) the shear stress in members with open thin-walled cross sections, Figure 12.19. We shall assume that the individual segments of the open cross section are long and thin, and that the shear stress will be estimated at locations remote to external and internal corners (rounds and fillets). Then,

$$S_{xt} = 3\frac{M_{xx}b_j}{\sum_{i}^{n} ab_i^3}$$

in which b_j pertains to the thickest of the i segments.

Example

Estimate the maximum shear stress developed when the member below experiences a twisting moment of 300 Newton-meters.

$$S_{xt} = \frac{3x300x12x10^{-3}}{(150x12^3 + 100x6^3)18^{-12}} = 38.5 \text{ Mpa}$$

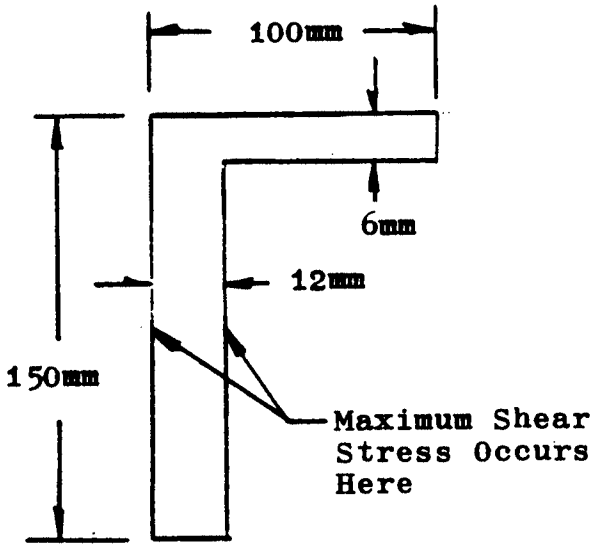

Open thin-walled cross section for numerical example above

Figure 12.19 Typical open thin-walled cross sections. The slit circular member is analyzed as a rectangular cross section with width ($2\pi r$) and thickness t. (The torsional rigidity of this cross section is quite small compared to that for a seamless tube.)

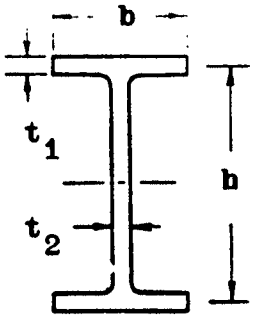

(a)

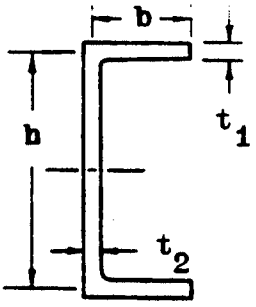

(b)

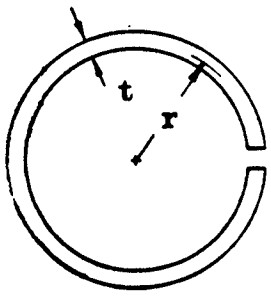

(c)

Exercise:

Estimate the maximum shear stress for the slit circular cross section as a fraction of the corresponding stress in a seamless tube.

WELDED MEMBERS

The actual state of stress in a fillet weld is so complex that welds are sized on the basis of elementary calculations coupled with allowable stresses established by Codes (based on both experience and test data). We now present the elementary weld stress calculations that are analogous to nominal torsional stress calculations for round members.

Elementary Analysis:

Consider Figure 11.20. The force and moment statically equivalent to force $\vec{P}$ in (a) appear in (b). Considering now only the moment (because the shear force was considered in Chapter 11), it creates a shear stress $\vec{S}_{z\theta}$ in a typical segment of the fillet weld of interest. If the bracket is assumed to be rigid-like, the strain in the weld is proportional to its distance from the center of rotation of the bracket (which static equilibrium indicates coincides with the centroid of the weld pattern). But this strain distribution assumption is identical to that in a round member under torsion. Hence, we obtain (for a Hookean material) the stress distribution

$$S_{z\theta} = \frac{M_{zz} r}{I_{RR}}$$

where $I_{RR} = I_{XX} + I_{YY}$ and r is the distance to the location of interest in a given weld (in the basal plane).

Figure 11.20 Typical welded bracket experiencing a twisting moment (about the centroid of the weld areas).

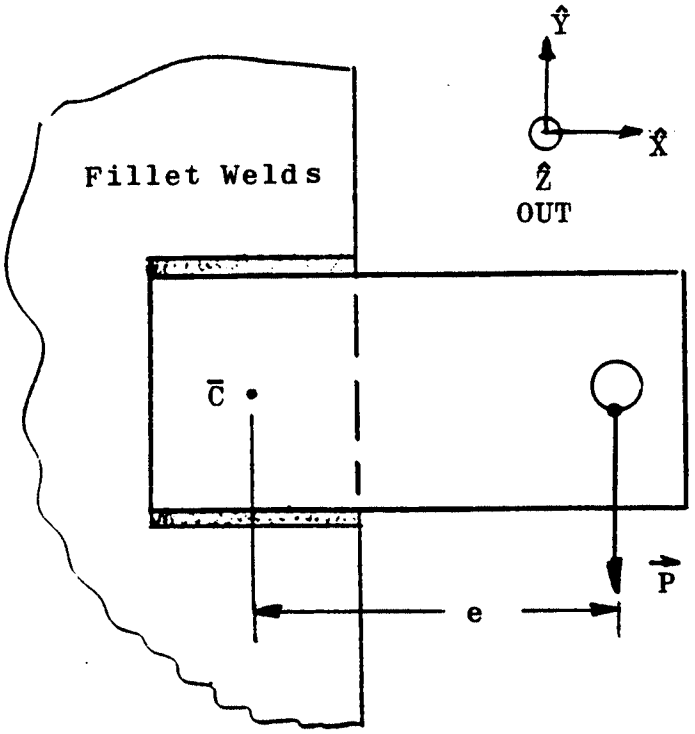

(a) Typical Application. $\bar{C}$ = centroid of weld area in the basal plane.

Typical Segment of Fillet Weld

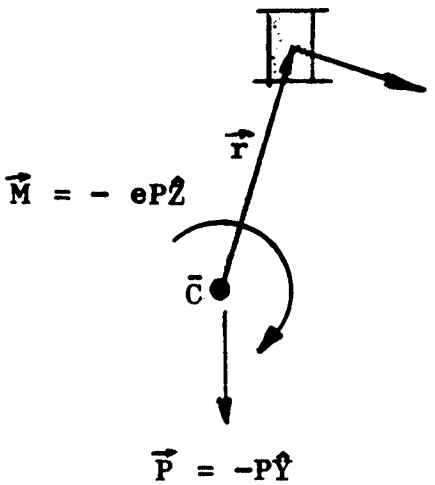

(b) Stress distribution assumed linear in r.

Exercises:

1. Compute the maximum shear stresses $S_{ne,max}$ for each weld detail and indicate by the appropriate sketches the directions of the maximum shear stresses (for subsequent vector addition).

(a)

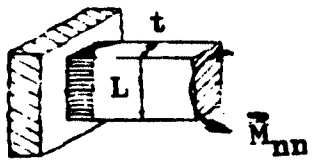

(t=2w)

(b)

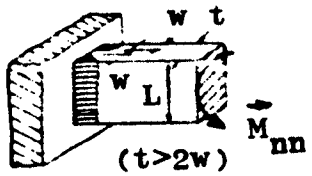

(t>2w)

(c)

(d) 

2. Compute the maximum values of the shear stresses $\vec{S}_{ne,max}$ pertaining to the welded brackets given in Sketches One and Two. Start your stress analysis by stating the statically equivalent force and moment acting at the centroid of the weld areas in the basal plane. One component of the moment theoretically generates a stress distribution that is analogous to nominal torsional stress distributions in round members. Let P = 1500 Newtons and θ = 30 degrees unless stated otherwise.

(a) Sketch One
(b) Sketch Two, 3mm fillet welds
(c) Sketch Two, 6mm fillet welds

Sketch One

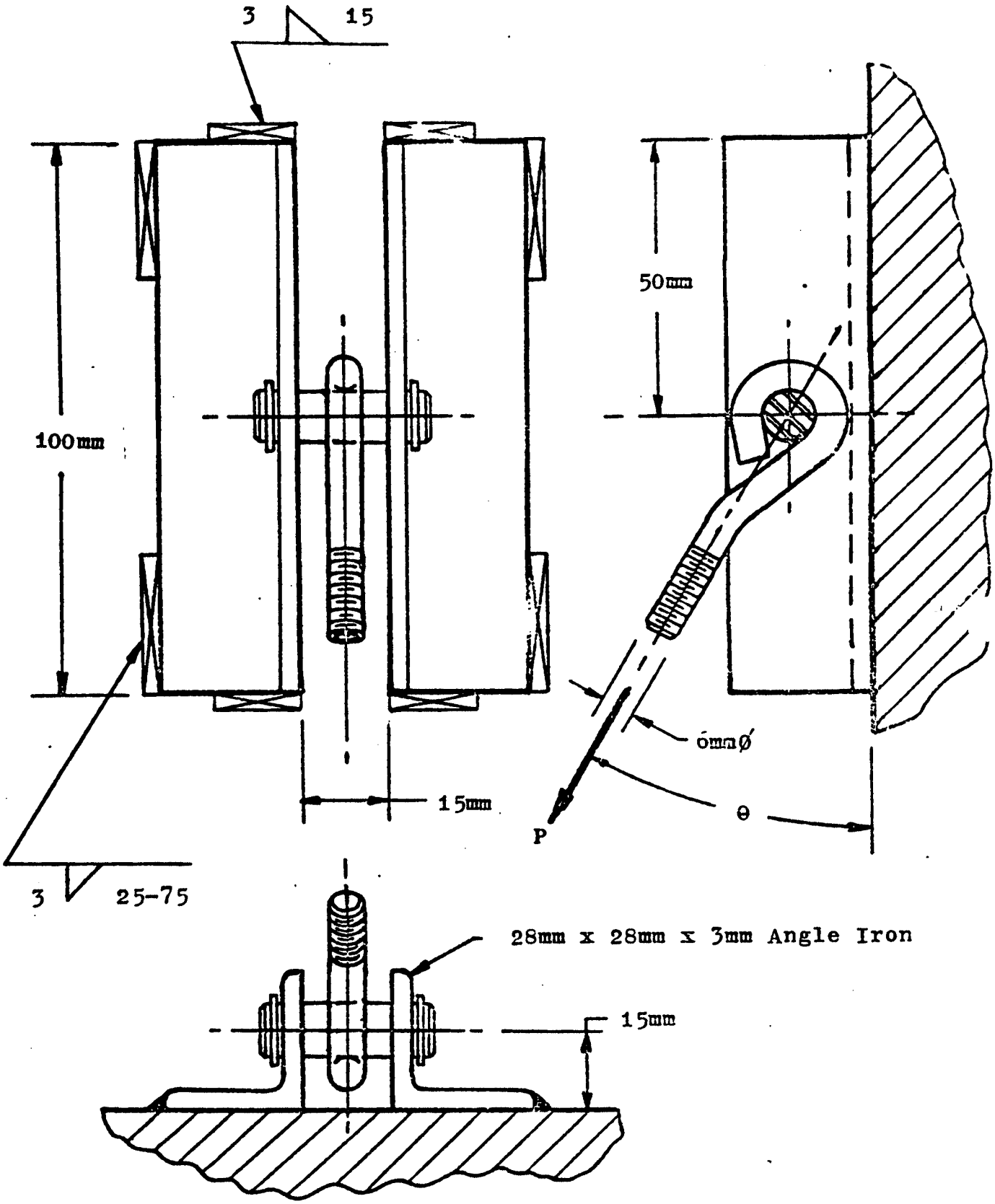
3
15
100mm
50mm
15mm
6mmØ
θ
P
3
25-75
28mm x 28mm x 3mm Angle Iron
15mm

Sketch Two

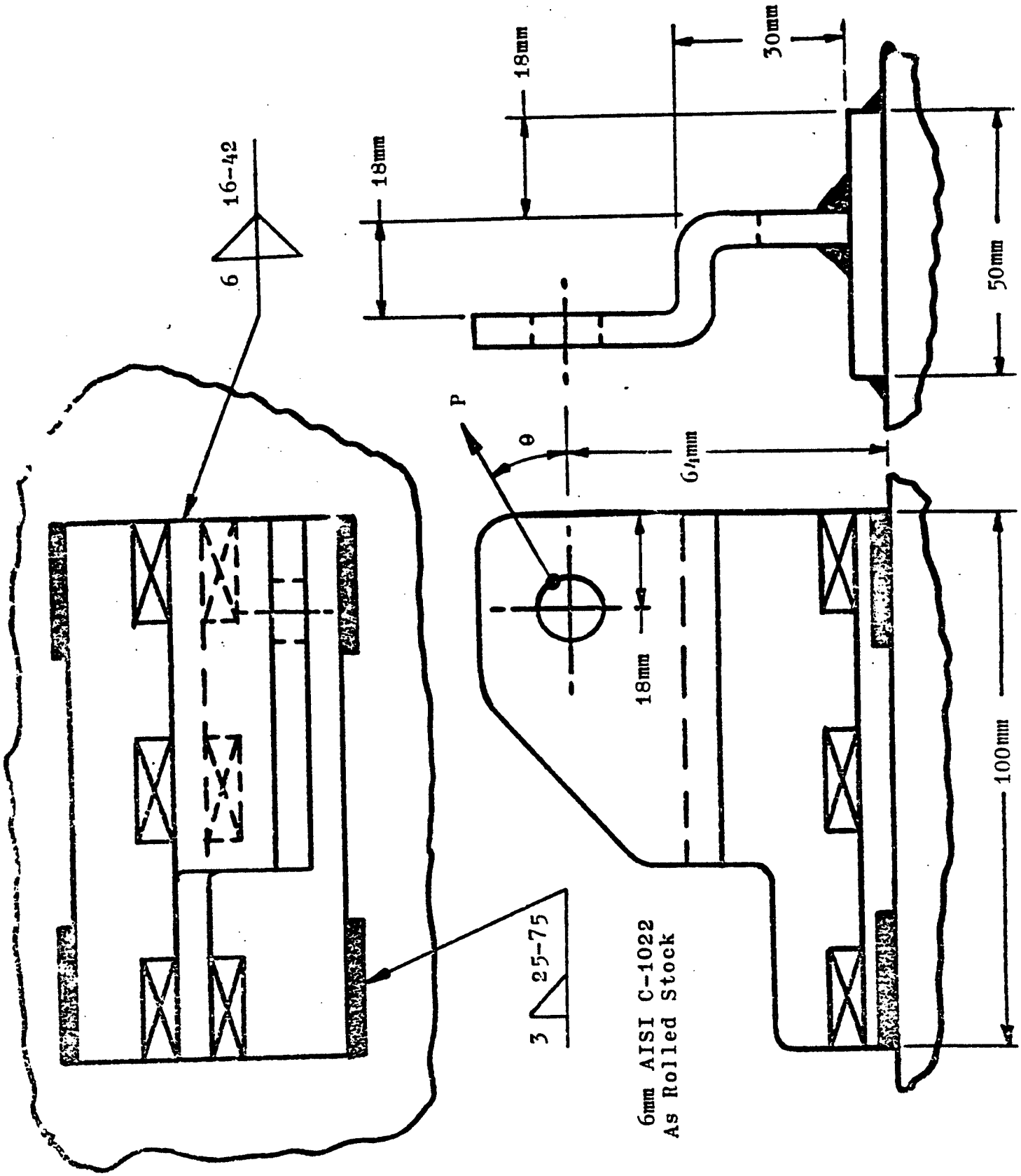
16-42
6
18mm
18mm
30mm
50mm
P
θ
61mm
18mm
100mm
25-75
3
6mm AISI C-1022
As Rolled Stock

BOLTED AND RIVETED MEMBERS

If we assume that the member is rigid-like and that each bolt or rivet is deformed proportionally to its distance r_i from the center of rotation (the centroid of the bolt or rivet pattern in the basal plane), then the analysis of bolted and riveted members is almost identical to that for a welded member. The primary difference is that I_{RR} is computed using the expression

$$I_{RR} = \Sigma A_i r_i^2$$

and we regard S_{ze} (S_{ne}) as being uniform over the entire bolt or rivet cross sectional area.

If the application of interest involves press-fit high-strength bolts, the assumption that each bolt actually resists the shear force computed may have reasonable credibility. Otherwise, alternative analyses based on alternative assumptions should be generated and evaluated.

Exercises:

Compute the shear stresses $\vec{S}_{ne,i}$ for each bolt in Sketches Three and Four. Start your stress analysis by stating the statically equivalent force and moment acting at the centroid of the bolt pattern in the basal plane. Let P = 1500 Newtons and θ = 30 degrees unless stated otherwise.

(a) Sketch Three

(b) Sketch Four

Sketch Three

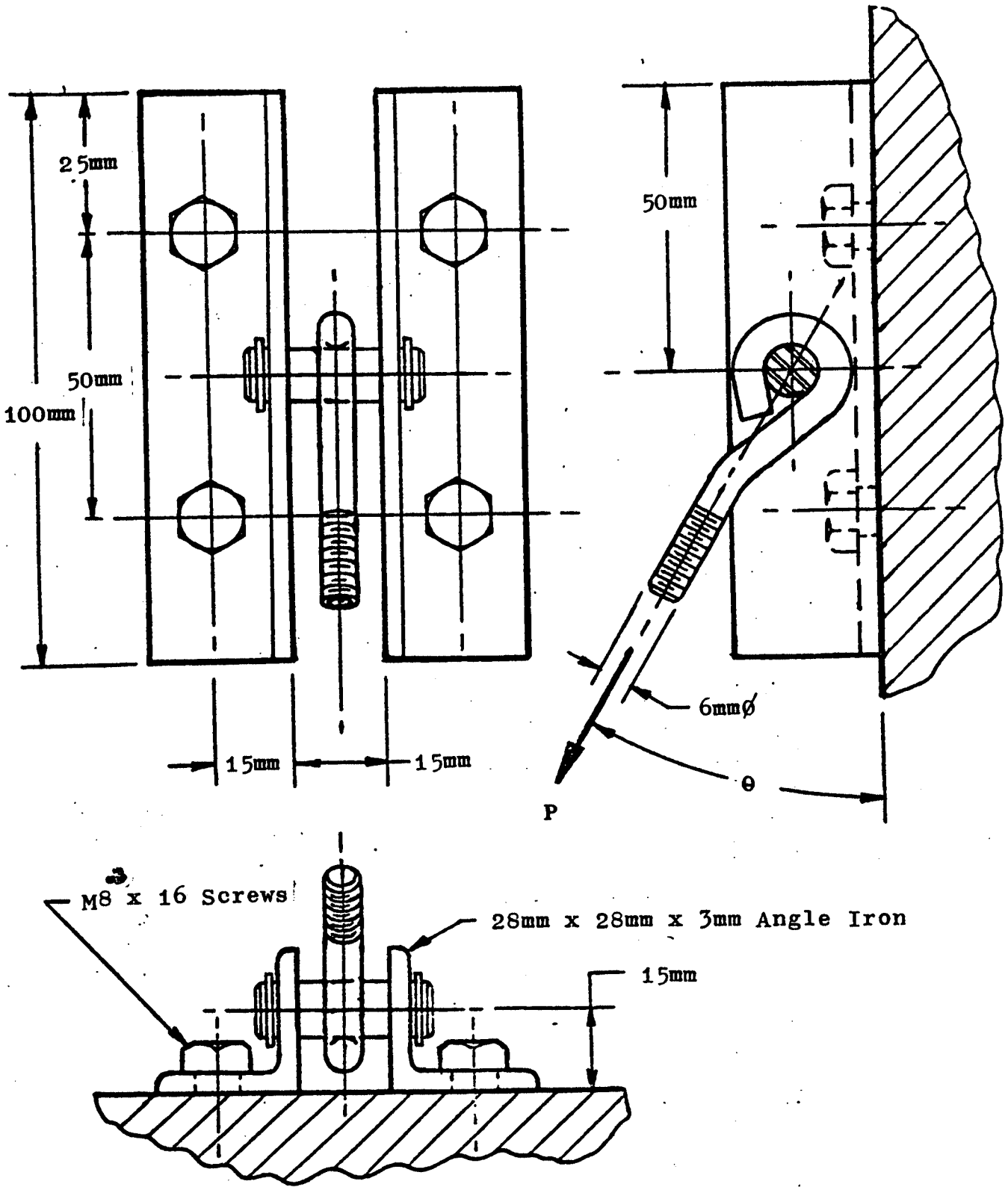

Sketch Four

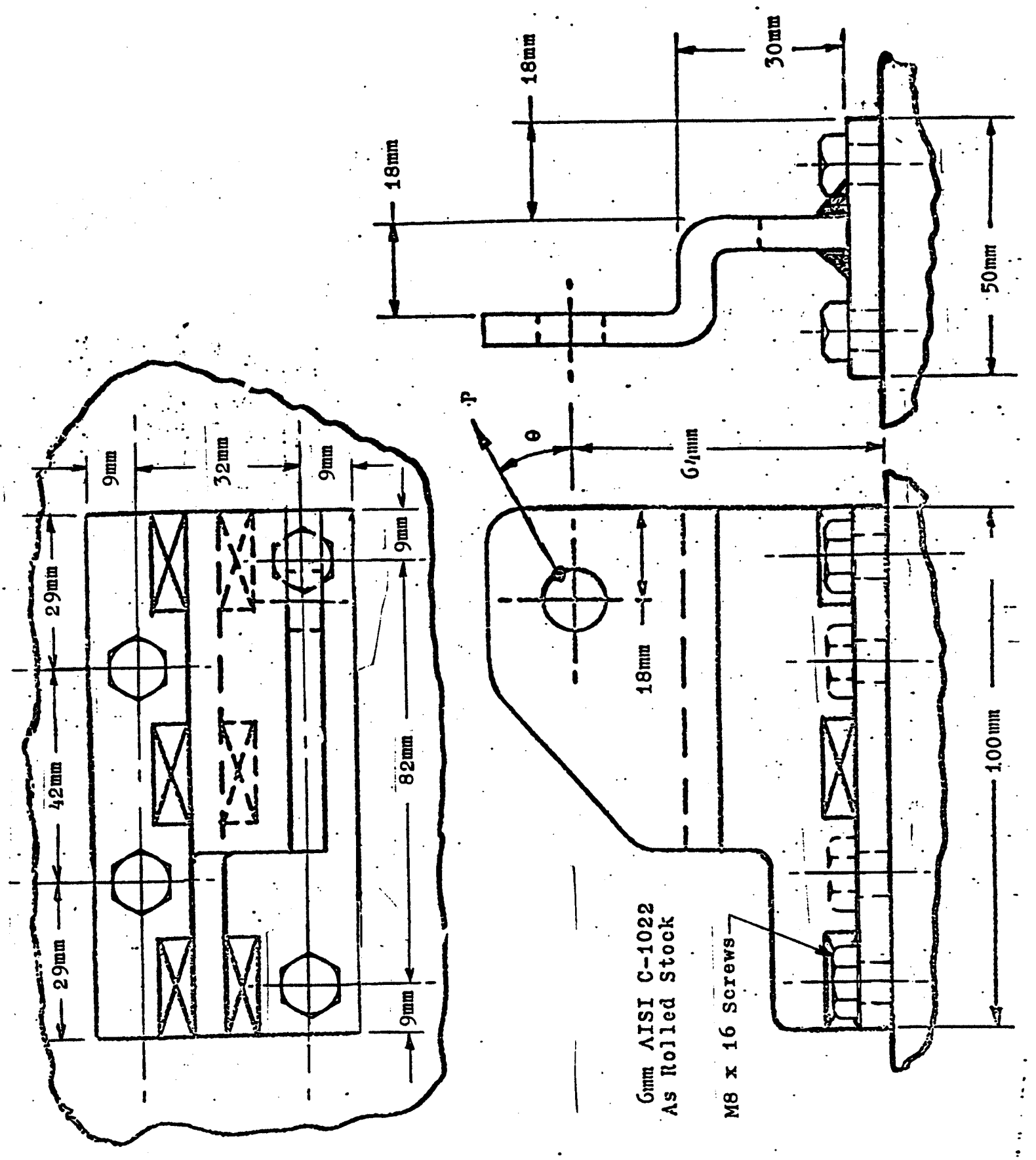
18mm
18mm
30mm
50mm
P
θ
61mm
9mm
32mm
9mm
9mm
29mm
42mm
29mm
82mm
9mm
18mm
100mm
6mm AISI C-1022
As Rolled Stock
M8 x 16 Screws